TURBULENT VELOCITY DISTRIBUTION IN FREE VORTICES ABOVE A VERTICAL DRAW-OFF

by

ALAA HUSSEIN KADOURY, M.Sc.

A thesis submitted in partial fulfilment

of the requirements for the degree of

DOCTOR OF PHILOSOPHY

of the

COUNCIL FOR NATIONAL ACADEMIC AWARDS

Department of Building and Civil Engineering,

Liverpool Polytechnic

February 1986

VOLUME ONE

TO MY BROTHER

ABSTRACT

Alaa H. Kadoury

Turbulent Velocity Distribution in Free Vortices above a Vertical Draw-off

The investigation was carried out on free surface vortices formed in an open topped cylindrical chamber of 600mm diameter, having a central draw-off pipe set level with the base. Water entered Tangentially through a vertical slot of adjustable width, no vanes or other directional aids being involved.

Tangential and radial velocities and their turbulent fluctuations were measured throughout the vortex, using draw-off pipes of 3 diameters. A single component Laser Doppler Anemometer in forward scatter mode was used, data collection and evaluation of mean and RMS velocities being performed simultaneously on a micro-computer.

Analysis established that for a considerable part of the vortex, turbulence is negligible, and circulation is constant. Closer investigation of a region adjacent to the outlet pipe shows that radial accelerations are important and is designated a zone of Accelerating Flow. The extent of this region is estimated, and values of eddy viscosity and Reynolds stresses calculated using hydrodynamic theory.

A dimensionless form of relationships between Circulation , Discharge, Outlet size and Depth is also submitted as a design aid.

ACKNOWLEDGEMENTS

The author wishes to express appreciation to Mr. C.Dyson, Principal Lecturer in Civil Engineering who supervised the research, provided encouragement at all stages of the work, gave generously of his time and assistance when help was needed, and reviewed the preliminary manuscript.

In particular, acknowledgments are made to the IRAQI Government Ministry for Higher Education and Research for the scholarship throughout the required period, and also to the technical staff of the Department of Civil Engineering Liverpool Polytechnic for their excellent workmanship in the construction of the model chamber.

CONTENTS OF VOLUME ONE

CHAPTER THREE

SURVEY OF MEASUREMENT TECHNIQUES

CHAPTER FOUR

MATHEMATICAL FORMULATION

CHAPTER FIVE

EXPERIMENTAL WORK

CHAPTER SIX

RESULTS AND DATA ANAYLSIS

CHAPTER SEVEN

DISCUSSION

CHAPTER EIGHT

CONCLUSIONS

LIST OF TABLES

LIST OF FIGURES

Figures 6-7-1 to 3	Contours of the Radial velocity Component at <0.5 cm/sec.
Figures 6-8-1 to 3	Dimensionless relationships

CONTENTS OF VOLUME TWO

LIST OF FIGURES

LIST OF TABLES

NOMENCLATURE

b	Breath of the inlet channel
d	Outlet pipe diameter
D	Vortex chamber diameter
F	Body force
F1,F2,...etc.	Mathematical functions
F_*	Dimensionless parameter
F•	Dimensionless parameter
g	Gravitational acceleration
h	Static head / water depth in the vortex chamber
K	Constant
p	Pressure (instantaneous or mean)
p'	Pressure fluctuation
Q	Volume flow rate
R	Reference radius
r	Radial coordinate
ra	Air core radius
ro	Radius of the outlet pipe
r•	Radial boundary of the Accelerating Flow region (III)
r_*	Radial boundary of the Tangential Flow region (II)
Re	Reynolds number ($V R/\nu$)
Re_*	Reynolds number at r_*
Re•	Reynolds number at r•

u	Radial velocity component (instantaneous or mean)
u'	Fluctuating radial velocity component
$\overline{u'v'}$	Reynolds shear stress
V	Reference velocity
v	Tangential velocity component (instantaneous or mean)
v'	Fluctuating tangential velocity component
v_*	Tangential velocity component at r_* (instantaneous or mean)
$v^\bullet$	Tangential velocity component at $r^\bullet$ (instantaneous or mean)
w	Axial velocity component (instanteous or mean)
w'	Fluctuating axial velocity component
z	Axial coordinate
$z^\bullet$	Axial boundary of the Accelerating Flow region(III)
Γ^*	Circulation at $r_* = v_* r_*$
$\Gamma^\bullet$	Circulation at $r^\bullet = v^\bullet r^\bullet$
Γ_2	Circulation in the Tangential Flow region(II)
Γ_3	Circulation in the Accelerating Flow region(III)
δ	Thickness of the boundary layer
ε	Eddy viscosity
ν	Kinematic viscosity
τ	Shear stress
θ	Cylindrical coordinate

CHAPTER ONE

INTRODUCTION

1-1 General

Rotations within a body of fluid occur wherever the boundary or boundary conditions change sufficiently rapidly.In fluids containing no suspended particles,vortices so generated are invisible when formed deep within the fluid, but nevertheless abstract a significant amount of energy from the system.

In liquid systems with a free surface, vortex motion becomes apparent when a small depression appears in the surface,greater relative intensity being indicated by the depth of the depression. In the case of a pipe situated so as to withdraw water from a channel or a sump, the ultimate condition is reached when the depression at the centre of the rotation extends into the pipe , so causing the discharge to be an air/water mixture.

The nature of the vortex motion being to dissipate energy , it then becomes the responsibility of the designer of systems or structures where vortices are likely to form to attempt to prevent their development. It is apparent that vortices without air core must by their very nature reduce the flow rate through a pipe draw-off system, below that which would occur at the same energy without these undesirable rotational tendencies. Consequently it

follows that to attain the same discharge with air core as would occur without,the upstream energy level would need to be increased. It is also apparent that the greatest discharge occurs when fluid motion at entry to a pipe system is radial/axial rather than rotational. Radial piers are often installed at the approaches to a bell-mouth over-flow from a reservoir so that it will operate at minimum head conditions under all important circumstances. Similar guidance arrangements in pumping systems are installed to prevent air being ingested to the detriment of the machinery and consequent increases in operating and maintenance costs.

Circumstances exist in which rotational flow is encouraged, prevention of the rotation not being the object of the design process. The most common of these applications is the conical tower used to separate and classify air, water,or oil borne materials. Additionally use is also made of the concept within some sewer systems. Vortex brakes are installed to reduce flooding towards the outfall of a sewer, by throttling the inflow from tributaries and hence utilizing pipe storage in the smaller diameter pipes at an early stage during the storm hydrograph. Vertical pipes fed rotationally at the top are occasionally used to ensure that flow being transferred to a lower level sewer clings to the wall of the pipe,so preventing the formation of a plunging jet with the possibility of structural damage at the lower level. The design

methods employed in the cases instanced are based upon practical experience, checking of modifications usually being estimated by laboratory testing of scale models, the interpretation of which can possibly be more subjective than engineers prefer due to the well known incompatibility of the criteria for satisfaction.

This investigation was initiated during model testing of a storm-water sewer overflow using simulated sewage particles. The design incorporated the usual overflow weirs,with floating materials being retained by scum-boards. During testing it was found that vertical stand pipes connected through the base of the chamber facilitated the collection of these more buoyant particles. A literature survey to locate references relating to the hydraulic performance of such intakes did not discover any information likely to enable the basic geometrical parameters to be established. A fundamental requirement to enable such a device to be designed is knowledge of the flow patterns in close vicinity to the outlet pipe, so that the depth of operation can be established.

The literature survey, discussed later, produced reports from many investigators who experimented in closed cylindrical containers. Generally fluid was fed in tangentially at the perimeter and withdrawn axially at the base, the whole system being symmetrical. These types of apparatus were totally enclosed, the cylinders being fitted with lids, with no central air column being permitted to form. In these instances the assumption generally

made was that rotation of the fluid was about the axis of symmetry. Other experimenters introduced guide vanes around the periphery of the cylinder to establish symmetrical conditions , and provide some form of control on circulation. Cylinders permitting free surface flow conditions have also been used, guide vanes being utilized widely to stabilize the rotation. Measuring techniques employed have been many and varied, including current meters and time-lapse photography, together with other optical arrangements.

It was considered that in general the experimental work covered in the literature survey tended to be designed to enforce circulation patterns on the flow in order to facilitate measurement techniques, but which by so doing produced conditions which were possibly rather artificial. This experimental work was intended to be free of these constraints,as described later.

1-2 Measurements

Observation and measurement of velocities in vortex flow has always been difficult since the introduction of any device, however small, into the flow is likely to trigger instabilities, specially at the point of measurement. The degree of interference depends on the form and size of the particular instruments (pitot-tubes,propeller-type current meters and hot-wire anemometers) and especially on the proximity of solid or fluid boundaries. In some cases photography may be employed instead ,by photographing the movement of solid particles floating or sus-

pended in the fluid, in other cases flow visualization by dye injection has been used and in some other cases simple optical arrangements (microscope) , smoke injection and taft screens have been used particularly the last two to enable visualization of trailing vortices from the wing tips of aircraft. Some details of each of these methods will be given in the following chapters. All the above mentioned techniques are either lengthy or inaccurate or involve interference with the flow. The use of Laser Doppler Anemometry enables the measurement of the local, instantaneous velocity of tracer particles suspended in the flow to be made. The flow regime is not obstructed, and velocity profiles are quickly obtained. Laser Doppler Anemometer using frequency shifting techniques enables the direction as well as the magnitude of the velocity to be determined. Control and focussing of the laser at the required point requires lenses and prisms of high optical quality to produce measuring systems utilising the reference beam, dual beam and the two scattered beams systems.

In the reference-beam or "local oscillator heterodyning" mode, the Laser beam is split into an intense scattering beam and a weak reference beam. The reference beam is directed on to a photo-cathode where it beats with light scattered from the strong beam by particles moving with the flow; the frequency of the scattered light will be altered by the Doppler effect and the in-

terference with the reference beam provides a frequency difference which is directly proportional to the particle velocity.

The "dual-beam" or fringe mode (the system used by the author) uses two intersecting light beams of equal intensity to produce a fringe pattern within their volume of intersection. As each particle crosses the fringes, the intensity of light scattered onto the photodetector rises and falls at a rate directly proportional to the velocity.

In the third optical arrangement a single focused Laser beam is directed into the flow and light scattered by a particle in two directions is collected symmetrically about the system axis. When the scattered beams are combined, the relative phase of their wave fronts depends on the distance of the particle from each light collecting aperture; hence as the particle moves across the beam the scattered light interferes constructively and destructively leading to a light intensity at the photo-cathode which fluctuates at the Doppler frequency.

1-3 Research Objective

Previous investigators identified various regions having different flow characteristics, but with no precise indication of their relative proportions. It had been suggested that the area adjacent to the outlet had a major influence on the discharge. It was proposed to investigate this area more intensively using laser techniques, and the large amounts of data expected used to provide

closure conditions for the solution of the classical hydrodynamic equations.

Using the results of these theoretical analyses it was hoped to propose design criteria for engineering use.

CHAPTER TWO

LITERATURE SURVEY

2-1 Introduction

In this chapter, a detailed account of the most relevant previous research is presented. The work is presented in chronological order and particular attention has been focused on works which have investigated air-entraining vortices. The terminology used and opinions expressed throughout this section are those of the particular writer or referenced contributor concerned.

The final comments and opinions will be presented in chapter eight.

2-2 EINSTEIN and LI (1955)

The elementary vortex flow of a viscous fluid with a vertical axis of symmetry and radial flow rate Qo toward a central drain opening of radius ro was treated by EINSTEIN & LI on the basis of certain simplifications of the Navier-Stokes Equations. The simplifying assumptions were as follows:

a) the flow is symmetrical about the axis of rotation of the cylindrical coordinate system (r,θ,z)

b) the axial velocity component, w, is negligible

c) the radial velocity component, u, can be approximated by the expression:

2-2-1 $$u = Qo/(2\pi rL) \qquad \text{for } r \geq ro$$

and

2-2-2 $$u = Qo(r/ro)^2/(2\pi rL) \qquad \text{for } r \leq ro$$

Where L is the depth of the vortex and $2\pi rL$ is the area of the cylindrical surface at distance r from the axis of the vortex. Equation 2-2-2 implies that the flow rate Q across this cylindrical surface is given by:

2-2-3 $$Q = Qo(r/ro)^2 \qquad \text{for } r \leq ro$$

That is, the velocity distribution across the bottom drain is assumed to be uniform. According to assumption (c), the small increase in water depth with increasing r can be neglected, as compared with the total depth , in the calculation of u . Assumptions (b) and (c) imply a contradiction , that can be resolved only through comparison with experimental results.

With these assumptions, the radial component of the Navier-Stokes equations simplifies to

2-2-4 $$u(\partial u/\partial r) - (v^2/r) = (1/\rho)\partial(p+\gamma Z)/\partial r$$

Equation 2-2-4 is valid for both $r \geq ro$ and $r \leq ro$ In both cases the viscous term turns out to be zero. When use is made of equations 2-2-2 and 2-2-4 the tangential component of the Navier Stokes Equations yields on the other hand:

$$2\text{-}2\text{-}5 \qquad u(\partial u/\partial r) + (uv/r) = \nu[(\partial^2 v/\partial r^2) + 1/r(\partial v/\partial r) - (v/r^2)]$$

whilst the axial component shows that the pressure distribution is hydrostatic in the vertical direction.

In order to integrate equations 2-2-4 and 2-2-5 the value of u was introduced from equations 2-2-1 and 2-2-2 with the use of the constant A ($A = Qo/(2\pi L\nu)$) and imposing the condition that at r = ro the two solutions (for $r \geq ro$ and $r \leq ro$) must yield the same value of both the velocity and the shear stress. The later condition implies equal values of the derivative $\partial(v/r)/\partial r$ at r = ro. One then obtains the following expressions for the product of the tangential velocity v and the radial distance r as a function of r:

$$2\text{-}2\text{-}6 \qquad rv/rovo = K1/(1 - K2) \qquad \text{for } r \leq ro$$

where

$$K1 = 1 - e^{-(A/2)(r/ro)^2}$$

$$K2 = e^{-A/2}$$

and

2-2-7 $$rv/r_*v_* = [\ K3(1-K4)/(1-K5)]+K6 \text{ for } r \geq ro$$

$$K3 = [(rv/rovo) - (ro/r_*)^{-(A-2)}]$$

$$K4 = (r/r_*)^{-(A-2)}$$

$$K5 = (ro/r_*)^{-(A-2)}$$

$$K6 = (r/r_*)^{-(A-2)}$$

where the tangential velocity vo at a distance ro from the axis is given by

2-2-8 $$rovo/r_*v_* = (A-2)(1-K2)/[A(1-K2(r/r_*)^{(A-2)} - 2(1-K2^{-1})]$$

Here v_* is a reference tangential velocity at a distance $r_* > ro$ from the axis, which determines (or is determined by) the strength of the vortex.

The results in equations 2-2-6, 2-2-7 and 2-2-8 are valid for $A \neq 2$. In the case where A = 2 and imposing the same boundary condition

2-2-9 $$rv = [A-2(1-K2)(1-r^{-(A-2)}]/[A(\ 1-K2ro^{(A-2)})-2(1-K2)] + r^{-(A-2)}$$

Equation 2-2-9 is proposed as describing vortex flow under laminar conditions. The values of A determined from analysis of the experimental results were much smaller than those given by the assumption that $A = Qo/(2\pi L\nu)$ Einstein & LI attributed this discrepancy to possible turbulence effects and suggested using the following equation:

2-2-10 $$Ae = Qo/(2\pi L(\nu+\varepsilon))$$

where ε is the eddy viscosity. Equation 2-2-10 is valid if:

a) the turbulence is proportional to the shear stress, then its affects compliment the viscosity.

b) ε is constant in the following equation:

2-2-11 $$\varepsilon r\partial(v/r)/\partial r = -u'v'$$

2-3 DENNY D.F. & YOUNG G.A (1957)

In their paper they tried to find the factors affecting the formation and effects of vortices and swirl in pump intakes. These factors were:

1- Critical submergence & intake velocity

From their experimental findings they conclude that there is one region at low intake velocities where the

critical submergence is very dependent on velocity through the intake, and another at high intake velocities where the critical submergence is not very dependent on velocity.

2- Critical submergence and the strength of the rotational flow

It was found that the rotational velocities were greatest when the water entered through half the width of the sump and this condition caused the most severe vortices, requiring a critical submergence of 15 draw off pipe diameter to prevent air-entrainment. With the water entering over the whole width of the sump the critical submergence was only 3.5 diameters even at high velocities. A fourfold change in the critical submergence at high velocity was affected merely by varying the angular momentum of the approaching flow about the intake.

3- Boundaries of approaching flow

It was found that as the intake was raised from the floor the critical submergence decreased, although the actual water depth increased considerably. Also the critical submergence at a given velocity was greatest when the intake was near the centre of the sump and least when the intake was close to the wall. The critical submergence was independent of wall clearance when this exceeded 10

pipe diameters and was approximately proportional to wall clearance when this was less than 5 diameters. Experiments showed that the shape of the intake had very little effect on vortex formation. Upward facing and downward facing vertical intakes behaved very much alike, but with horizontal intakes the disposition of the intake relative to the vortex zone in the sump appeared to be important.

A series of experiments was carried out to determine the effect of a number of variables on the intensity of the swirling flow in the intakes. It was clear that the distribution of the tangential component of the velocity across the pipe inlet could be approximated to that of a free vortex (i.e. velocity inversely proportional to radius) while further along the pipe the swirl corresponded more nearly to solid body rotation (velocity proportional to radius). It was also found that swirl angles were independent of the flow, but were considerably affected by the depth of water in the sump.

Denny & Young suggest that when vortices are discovered in existing installations, remedies that may be employed are:

a) those which obstruct the free rotation of the water in the neighbourhood of the intake.

b) those which deflect the tail of the vortex away from the intake.

Denny & Young used small-scale models of several existing or proposed pump installations and some hydroelectric schemes to investigate the possibilities of air-entrainment at such intakes. Their conclusions were:

1- Air-entraining vortices and swirling flow at the intake both arise from rotations in the water supplying the intake, the magnitude of which depends on the position of the intake relative to the direction and boundaries of the approaching flow.

2- In extreme cases, over 10% of the flow entering the intake consists of air and swirl angles up to 40° can be realised.

3- Severity of both air-entraining vortices and swirling flow is diminished by :

a) reducing the strength of the rotational flow in the approaching water.

b) increasing the area of the intake.

c) increasing the depth of water.

d) siting vertical or slightly sloping walls close to the intake.

4- The only remedies that are equally satisfactory for these troubles is the use of guide vanes.

5- For intakes up to 3ft in diameter, models larger than 1/16 scale are capable of providing accurate quantitative

data provided that the velocities in the model are equal to those in the prototype. The laws applying to intakes larger than 3ft are not completely understood. If no air-entrainment is apparent, swirling is likely to be significant.

2-4 STEVENS J.C. & KOLF R.C.(1957)

Stevens & Kolf's work was to study the behaviour of a vortex chamber and to use it to divert sewage from combined sewers into intercepters. They applied the differential equation which gives the pressure change normal to a stream line for a flow in a curved path

2-4-1 $\partial P = \rho(v^2/r)\partial r$

with Newton's second law applied to irrotational flow in a free vortex

2-4-2 $\partial(rv)/\partial t = 0$

2-4-3 $v = K/r$

2-4-4 $\Gamma = 2\pi rv$ (circulation)

substituting equation 2-4-3 in 2-4-4

2-4-5 $\Gamma = 2\pi K$

By applying the continuity equation to the radial flow, with y the vertical distance between the flow lines assumed constant and u the radial velocity then;

2-4-6 $$Q = 2\pi ryu$$

and

2-4-7 $$u = K1/r$$

With these assumptions,both u and v have the same inverse relation to the radius. Thus the stream lines are equiangular and are theoretically logarithmic spirals. Utilizing equations 2-4-1,3,and 7 with the Bernoulli Theorem gives

2-4-8 $$(P1 - P2)/w = (K3^2/2g)[(1/r2^2) - (1/r1^2)$$

where

$$K3^2 = K^2 + k1^2$$

It is to be expected that for free vortex motion through a horizontal orifice, equation 2-4-8 above will be altered because:

a- the distance y is not constant

b- viscous forces predominate in the region near the orifice and completely overwhelm the effects resulting from a theoretically free surface boundary.

Stevens & Kolf also showed that the discharge coefficient could be related to the shape and character of the boundaries :

2-4-9 $$C = f(d/b , Rn, v)$$

Where C is the discharge coefficient

d is the orifice diameter

b is the diameter of the tank

Rn is Reynolds number = vd/ν

Vn is the vortex number = $\Gamma/(d\sqrt{2gh})$

Their experimental work consisted of tests made in two different tanks of 180 and 360 cms. diameter and depths of 45 and 60 cms. Water was admitted to the tanks at four points around the periphery to ensure uniform conditions of radial flow. In order to induce a greater degree of vorticity a ring with guide vanes was constructed. Surface profile measurements were taken by the use of a moving point guage incorporating a special internal caliper which could be lowered into the vortex air core to measure its diameter.

The circulation was determined from the water surface profile measurements, by using equation 2-4-5 and the theoretical equation for an assumed hyperbolic water surface.

2-4-10 $$y = K^2/(2gx^2)$$

where x and y are coordinates of a point in the fluid.

Stevens & Kolf showed that their theoretical assumptions were in close agreement with the actual measurements when $x \geq d$. Using set of curves for Cd vs. Vn for different values of d, they proposed the following straight line relationship between Cd and Vn:

2-4-11 $$Cd = 0.686 - 0.218Vn \qquad (\text{for } 0.8 \leq Vn \leq 3.14)$$

An approximate coefficient of discharge for vortex flow through a horizontal sharp-edged orifice could be found directly from curves for values of $0 \geq Vn \leq 0.8$.

2-5 HOLTORFF G.(1964)

Holtorff presented a solution to determine the surface profile of a free vortex by integrating the second Navier Stokes equations under the following assumptions

1-Negligible average vertical velocity component,

2-Uniform axial velocity in the drain opening,

So for $r \leq ro$

2-5-1a $$rv = rovo(K1^{(r/ro)^2} - 1)/ (K1-1)$$

for $r \geq ro$

2-5-1b $$rv = [(rovo - K2)(1 - K3)/(1 - K3)] + K3$$

in which

2-5-2a $$rovo = (2-A)(K1-1)/(A(1-K1.K2 + 2(K1-1))$$

2-5-2b $$K1 = e^{-(A/2)}$$

2-5-2c $$K2 = ro^{2A}$$

2-5-2d $$K3 = r^{2A}$$

and

2-5-3 $$A = Qo/(2\pi h\nu)$$

Where r is the distance from the drain

v is the tangential velocity at r

ro is the radius of the drain

vo is the velocity at the drain

h is the water depth

Q is the discharge

ν is the dynamic viscosity

In equations 2-5-1a and 2-5-1b the variable moment of momentum depends on the initial moment vi.R, its value at the drain diameter voro., and a dimensionless parameter A defined by equation 2-5-3.

Holtorff showed that by integrating the first Navier Stokes Equations under these same two assumptions, two relations for the regions r≥ro and r≤ro are obtained, from which the water surface profile can be determined. For r≥ro and A >10 the following expression can be used :

2-5-4 $$h = H - (u^2/2g) - g(1-K1)^2/2g$$

(Where H is the specific energy at inlet)

For r≤ro the integration is not possible in a closed form, but when expanded into a series and integrated term by term

2-5-5 $$\Sigma = \int (v^2/r)\ \partial r(K1-1)^2 ro^2/(ro^2\ vo^2)$$

The Σ in equation 2-5-5 of the very slowly converging and alternating series is made graphically which shows curves of Σ against A for values of r/ro. The final solution for the free surface in the area r ≤ro is given by:

2-5-7 $$h = Ho - (u^2/2g) + [vo^2/\ g(1-K1)^2]\Sigma$$

where Ho is the specific energy at outlet.

2-6 ANWAR (1965)

Anwar in this paper presented a theoretical approach supported by experimental work for the formation of a vortex with an air-core

at the entrance of an outlet pipe discharging from a circular tank. He measured the tangential velocity and the water surface profiles, and he also calculated the discharge coefficient. His main findings were :

1- The tangential velocity is independent of height and varies only with the reciprocal of the radius from the axis of symmetry, and thus behaves as in a vortex in an inviscid fluid.

2- The condition of similarity for vortices is valid when the radial Reynolds number (i.e. the ratio of discharge per unit height of vortex to the kinematic viscosity) is greater than 1000.

Anwar also showed the influence of the boundary layer flow on the vortex motion. By artificially roughening the floor of the tank a weaker vortex was obtained having much reduced tangential velocities.

Anwar supported his theories by comparing his experimental results with theoretical analysis. It is shown that as the vortex core is approached, departures from the ideal form become more significant.

2-7 ANWAR (1966)

Anwar studied the formation of a weak vortex with a narrow air-core at an outlet. He found out that:

1-The axial velocity is practically zero at the axis of symmetry ,even when only a shallow dimple appears at the surface, but reaches its maximum at a distance about 0.75 times the outlet radius from the axis of symmetry.

2-The measured profiles of the tangential velocities followed that of a vortex in an inviscid fluid, increasing towards the centre with Γ constant but reaching its maximum value at a distance from the centre which was approximately the radius of the outlet pipe. Further towards the centre the tangential velocities decreased, and vanished at the axis of symmetry in the case of a dimple.

Anwar in his theoretical approach assumed that the motion in the vicinity of the vertical axis is

a-Steady

b-Axisymmetric

c-Laminar

Based on the above assumptions he derived three non-dimensional parameters from the equations of motion for incompressible fluid in cylindrical co-ordinate form, these parameters were :

2-7-1 $$C1 = Q / (r_o \Gamma_\infty)$$

2-7-2 $$C2 = Q / (\nu h)$$

2-7-3 $C3 = ro/h$

These parameters determine the formation of a shallow or deep dimple, the relation between these parameters and the limits of their application being shown.

2-8 GRANGER R. (1966)

Granger attempted to develop a mathematical model for an incompressible fluid in a steady three-dimensional rotational flow. He developed an exact differential equation of motion in terms of the circulation and the stream function for steady axisymmetric flow. He showed that this flow was related mainly by three dimensionless terms :

a) Local radial Reynolds number $Rr = Q / h\nu$

b) Rossby number $RN = QL/ro\Gamma$

c) Geometric ratio $GR = (ro/L)^2$

He also expressed the circulation and the stream function in a power-series expansion of the radial Reynolds number, which took the form :

2-8-1 $$\Gamma(\xi\eta) = \pi ro^2/\Gamma\infty[\Sigma\ (-a/4)^{n-1}\ (\eta^n\gamma^{(2n-2)})/(n1(n-1))$$

The stability of the solution is dependent upon the vorticity distribution $\gamma(\xi)$.

In addition he examined the following examples of rotational flow, based upon a specific distribution of vorticity along the axis of rotation:

a)The Rankin vortex , in which

$$2\text{-}8\text{-}2 \qquad \gamma = \Gamma\infty/(\pi r^2) \qquad \text{for } 0 \le r \le ro$$

Substituting equation 2-8-2 into 2-8-1 yields the circulation:

$$2\text{-}8\text{-}3 \qquad \Gamma o = (r/ro)^2 \qquad \text{for } 0 \le r \le ro$$

His diagrams show that for n>1 the flow is solid-body rotation, whereas for n<1 the flow is the potential vortex flow, and hence this motion is the circular Couette flow.

b) Three dimensional vortices

1-Rott's vortex

$$2\text{-}8\text{-}4 \qquad \gamma(\xi) = (\Gamma\infty/(\pi Ro^2))(\tanh 2/\sqrt{a})\ \xi$$

where $\xi = 0.44\sqrt{a}$

2-Alternative form of the three-dimensional vortex

With r and z as independent variables, an obvious alternative solution for the vorticity is the infinite power-series:

$$2\text{-}8\text{-}5 \qquad \gamma(r,z) = \Sigma_{m,n} a_{m,n} z^m r^n$$

with n = 0. (vorticity at the centre of rotation). Many vortex motions (Rott , Oseen,....etc) can be so analysed.

Expressions in closed form were derived for the axial and radial velocities by using the differential equation for the zeroth-order stream function Φo and the method of Frobenius, so for the axial velocity:

$$2\text{-}8\text{-}6 \qquad w/wo(\xi) = 1 - 1.699\ X^2 + 0.564\ X^3 + 1.826\ X^4 + ..etc.$$

and for the radial velocity:

$$2\text{-}8\text{-}7 \qquad u/wo(\xi) = X^{5/2}[1.1266 - 0.423\ X - 1.4688\ X^2 + 1.49\ X^3\ ..]$$
$$+ 0.5(a\eta\tfrac{1}{2})w'o/wo[1 - 0.5633X^2 + 0.114\ X^3 + 0.3672\ X^4]$$

The effect of viscosity on the motion was explained by including the First-order circulation (i.e. $\Gamma 1, \Phi 1, \Gamma 2, \Phi 2$ ..etc.) with the boundary conditions $\Gamma(\xi,0) = 0$, $\partial\Gamma(\xi,0)/\partial\eta = 0$

$$2\text{-}8\text{-}8 \qquad \Gamma 1(\xi\eta) = (\pi ro^2 1/\Gamma\infty Q)[a/4(\gamma - w'o - wo\gamma'\bullet)\eta/2i$$
$$- (a/4)^2(....etc.)$$

Finally Granger carried out some exploratory experiments to measure the vorticity,and axial and radial velocities in a steady laminar flow. The variation of vorticity and axial velocity along the vortex axis, the radial variation of vorticity, the radial distribution of the axial velocity, and the axial variation of core radius are illustrated

2-9 ANWAR (1967)

Anwar in this paper carried out his investigation to determine the effect of rigid boundaries on the formation of vortices. Experiments were conducted in a transparent cylindrical tank fitted with a central outlet pipe projecting vertically upwards through the base. The top of the tank was closed in order to produce vortices of high circulation. The tangential velocity was measured at a given level above the outlet pipe. Anwar reached the following conclusions:

1- The distribution of the tangential velocities corresponds to that of an inviscid fluid when $r \geq ro$ (ro is the radius of the outlet pipe).

2- The tangential velocities vary according to laminar motion when $0.0 \leq r \leq ro$.

3- The maximum tangential velocity occurs at about ro.

4- The maximum negative pressure occurs at the axis of symmetry.

5- Vortices can be suppressed by providing a rigid boundary at the free surface.

2-10 ZIELINSKI .P.B. etal.(1968)

Zielinski etal. carried out an experimental investigation to evaluate the effect of viscosity on vortex-orifice flow, their main findings were as follows:

1- The physical effects observed were

a) As the viscosity increases, the circulation decreases from inlet to outlet due to an increase in viscous shear.

b) As circulation decreases, the draw-down (fluid depth) decreases.

c) As the draw-down decreases, the air-core radius decreases, thereby increasing the area of the jet.

d) As the area of the jet increases, the coefficient of contraction increases, thus producing an increase in the over-all coefficient of discharge.

e) As the coefficient of discharge increases, the head must decrease in order to maintain a constant discharge rate.

2- At Reynolds number greater than 10,000 , the effect of viscosity can be neglected, the relation between the discharge coefficient and Kolf number V' using oil and water is shown.

2-11 ANWAR (1969)

Anwar in this paper attempted to apply different concepts of Reynolds shear stress in the momentum equation of motion in order to evaluate the eddy viscosity, and from that to determine the distribution of the shear stress across the turbulent region. He assumed that the shear stress term used in the momentum equation is proportional to the rate of strain, and from that he determined the distribution of eddy viscosity and shear stress across the turbulent region. The results showed that the shear stress and the eddy viscosity are negative in that region. Furthermore, by analogy with rectilinear flow, the eddy viscosity was calculated assuming it to be proportional to the rate of strain, and the universal constant χ . As an alternative he used Prandtl's expression for Reynolds shear stress proportional to vorticity. In this case the evaluation gave positive values for both the shear stress and the eddy viscosity across the turbulent region, although the magnitude of the shear stresses in both assumptions was the same but the eddy viscosity values differed. In addition to these two cases Anwar evaluated the eddy viscosity by assuming it to be proportional to vorticity from which the universal constant χ was again determined. In this case calculations showed the eddy viscosity to be constant across the turbulent region(the circulation values obtained not agreeing with the measured values).

The apparatus used was a transparent cylindrical tank of 90cms. internal diameter and 150cms. height. Water was led tangentially into the tank through eight nozzles at the circumference, arranged in two columns with four nozzles in each,set at right angles to one another. The tank was provided with a central outlet pipe of 100mm internal diameter and 270cms long set flush with the base. The top end of the tank was closed in order to produce vortices with high circulation. The top and bottom surfaces were roughened with expanded mesh to reduce the mass flow at the boundaries.

2-12 DAGGET L.L. etal. (1974)

Dagget etal. presented in this paper the effect of viscosity and surface tension on:

a)the incipient condition for vortex formation

b)the vortex shape

c)the vortex size.

They also studied the vortex effect on the efficiency of the outlet. To investigate the effect of viscous and surface tension forces on the formation of vortices, they varied Reynolds and Weber numbers while holding the other parameters (mainly geometric) at constant values. They accomplished that by using mixtures of water and glycerine and various grades of oil.

Their major findings were that:

1-This type of flow (free-surface vortex flow) is affected by both viscosity and initial circulation.

2-Surface tension does not appear to influence the type of flow.

3-The tangential velocity component is approximately constant throughout the depth, except in the boundary layer on the base.

4-The radial velocity component varies considerably with depth.

4-Flow toward the outlet is concentrated near the solid boundary, and the effects of the boundary roughness are therefore very significant.

2-13 AMPHLET M.B. (1976)

Amphlet investigated the formation of vorticies at a horizontal intake deriving non dimensional relationships from experimental data. His results show that:

1-Discharge coefficient varies with circulation number (ΓD/Q) and S/d (S is the critical submergence height, d is the internal diameter and Γ is the circulation) but is independent of b/d (b is the depression at the free surface).

2-Discharge coefficient for a given angle, increases with the increase in the intake height , but becomes less dependent on intake height when b is greater than 5d.

2-14 JAIN A.K. etal.(1978)

Jain ... etal. modelled the conditions of similarity for the onset of air-entraining vortices at vertical pipe intakes. They conducted their experiments using tanks of different sizes, varying the surface tension but keeping the viscosity constant by using iso-amyl alcohol (2%).They found that:

1-Surface tension has no influence on the critical submergence when the Weber number is greater than 120.

2-The critical submergence generally decreases with the increase in viscosity of the liquid because the circulation also decreases with increase in viscosity.

3-The critical submergence in the case of vertically downward pipe intakes is related to the circulation number, the Froude number and the viscosity parameter by the relation;

$$2\text{-}14\text{-}1 \qquad K\,(Sc/d) = 5.6\,(N_\Gamma)^{0.42}F^{0.50}$$

in which $K = f(N\nu)$ and attains a value of unity for $N\nu > 5 \times 10^4$ The relationship is valid for $1.1<F<20$. $0.1875<N_\Gamma<1.95$ and $N\nu>530$. [$N_\Gamma = \Gamma Sc/Q$ and $N\nu = g^{\frac{1}{2}}d^{3/2}/\nu$]

4-The Reynolds number R at which viscous effects become negligible is dependent on the Froude number F, the higher the Froude number, the greater Reynolds number for freedom from viscous influences.

2-15 ANWAR H.O. & AMPHLET M.B. (1980)

They determined some parameters relating the formation of a slender air core into the entry of a vertically inverted intake. The measured data indicated that the geometrical proportions of the intake are important. It also indicated that the effect of the kinematic viscosity and the surface tension on the measured values becomes negligible when the radial Reynolds number describing these effects is larger than 3000. This parameter is independent of the intake geometry and diameter, but not on the type of intake. Based on that and the measured data, non-dimensional parameters governing the formation of such vortices were suggested as:

1- $r^{\bullet}/H$, which represents the geometric similarity of a vortex with an air-core or a depression at the free surface ($r^{\bullet}$ is the radial distance measured from the vortex axis, at which a change in the velocity profile occurs). For the type of vortex presented here $r^{\bullet}$ was determined by an optical method ,H being the water depth above the intake. From the calculated values of $r^{\bullet}/H$, the following empirical relation was drawn:

2-15-1 $$r^{\bullet}/H = a + b/H$$

where a = 0.06 for the vertically inverted intake

and a = 0.054 for the horizontal intake.

b was described by the following empirical relation:

for a vertically inverted intake

2-15-2 $$b/H = (0.143/H)(B/D) + 0.89/H$$

and for a horizontal intake

2-15-3 $$b/H = (0.12/H)(B/D) + 1.0/H$$

2- $\Gamma r_{\bullet}/Q$ which they call the circulation number (Γ is the circulation calculated from $\Gamma = 0.86\ g^{\frac{1}{2}}\ r_{\bullet}^{2}/\ Ho^{\frac{1}{2}}$ where Ho is the total water depth).

3- Cd which represents the discharge coefficient calculated from $Cd = Q\ /(A\ \sqrt{2gH})$ where A is the area of the intake pipe.

4- Radial Reynolds number Rr which is calculated from $Rr = Q/(\nu H)$, where Q is the discharge through the pipe intake.

The results of the above approach give universal curves which are independent of the geometry .

Anwar and Amphlet in their analysis assumed that the flow is steady , axisymmetric about the axis of the vortex and that the fluid is incompressible. They also assumed that the flow in the

vortex is laminar and the occurrence of a slender air core does not bring any change in the velocity component profiles.

CHAPTER THREE

SURVEY OF MEASUREMENT TECHNIQUES

3-1 Introduction

This chapter will survey, review and give some description of several methods and techniques currently available or under development for the measurement of vorticity and vortex characteristics. More detail analysis of each method could be found in the reference cited.

3-2 Vane Vorticity Indicators

Vane-type (paddle or wheel type) vorticity indicators are well known for their use for demonstration purposes (Shapiro 1974). Utilization of these devices for quantitative velocity measurements received only scant attention for many years. Pertinent references relating to stream wise vorticity measurements are: McCormick etal. (1968), Barlow (1972), Holdeman and Foss (1974), and Zalay (1976). From comparison of circulation measurements around trailing vortices behind wings, obtained by several methods, Zalay concluded that the vorticity meter could underestimate the vortex strength, in some cases by over 50%, and noted that systematic calibration studies of this meter had never been performed. In his study ,calibration of the meter was accomplished by attaching a calibration collar in the form of a fixed vane swirl

generator to the device, just upstream from it. A relatively recent comparison of vorticity measurement carried out using Vane vorticity indicators with cross-wire velocity data (Wigeland etal. (1977) and Ahmed etal.(1976)). The vorticity meters used in this comparison were light weight, low moment of inertia miniature vanes, consisting of four perpendicular aluminum blades mounted on a rotating shaft fitted with teflon bushings and washers(jewel bearings were also used). Reduction of the friction was found to be essential to achieve consistent and repeatable measurements. The vanes were mounted directly upstream of a hot wire, which was used for detection of the passage of the blade wakes. Time averaged autocorrelation measurements of the wire output provided a signal from which the average speed of rotation of the meter could be calculated. A stable trailing vortex generated by two adjacent air foils set at equal but opposite angles of attack was used for the calibration, carried out by comparison with Cross- Wire velocity data.

3-3 Hot-Wire and Hot-Film Anemometry Systems

Transverse vorticity measurements in a streaming flow in the X-direction with the predominant vorticity vector in the Z-direction, using an array of hot wires, had been carried out by Foss(1979). The technique requires four wire arrays; a cross array at Z and an adjacent parallel array at $Z+\delta Z$ (Z direction

of the vorticity vector). Other pertinent references are Eckelmann etal.(1977), Kistler(1952), Willmarth(1979) and Wyngaard(1969).

3-4 Beam Reflection Method

The Beam Reflection Method attemts to determine the free surface profile of the rotating liquid, and utilizes a plane array of luminous points on a black background, either on the floor of the flow region of interest or on a plane above the free surface. The reflected image of the array on the free surface is photographed. To each different vortex depression or free surface shape there corresponds a geometric figure formed by the displacements of the images of certain points in the array. A relationship between these displacements and the circulation,Γ, of the vortex can be obtained under some simplifying assumptions. Experimental verification or calibration is necessary in all cases. Berge(1961) has pointed out certain difficulties which are inherent to this method, in particular in relation to the determination of the vortex axis.

3-5 Beam Refraction Method

This method has in fact been used by several investigators in the study of vortex formation problems (Berge(1965,1966), Levi(1972), Anwar etal.(1978), Amphlett(1976,1978), Anwar and Amphlett(1980), Anwar(1983)). The method uses the property of the light ray refracted at the air-water interface of the vortex. For an incident light beam formed by parallel rays and directed

normally to the free surface, the envelope of the rays (the caustic surface) is a vertical-axis surface of revolution, presenting a central shadowed region surrounded by an area of an accumulation of light rays. The intersection of the set of refracted rays with a horizontal plane thus produces a circular shadow, whose diameter can be shown to be related to the circulation, Γ, of the vortex. An analytical expression can be derived expressing this relationship (Berge 1965), but in practice it is necessary to calibrate experimentally this method for each value of the water depth (Levi(1972) and Anwar etal.(1978)).

3-6 Chronophotographic Flow-Visualization Techniques

A succinct account of the varied procedures which have been used for flow visualization can be found in Werle(1973), Macagno(1969) and Yang (1984).

Foreign particles or tracers suspended in the flow or floating on a free surface can be used to determine flow velocities using time-exposure photographs or comparison of successive frames of moving pictures. A clock must be included in the photos to determine actual time lapses accurately. Solid tracers used have included aluminum particles, spherical polystyrene beads, tellurium particles, glass beads, perspex powder, and mica chips. Liquid tracers which have been used are for example , condensed milk, a mixture of milk, alcohol, dye and water whose density and viscosity are close to those of water, diluted rhodorsil, ink, dye , carbon

tetrachloride, benzene solution containing powdered anthracene, and potassium permanganate. Gaseous tracers have included air bubbles produced naturally or artificially within the flow or injected by various means, and hydrogen bubbles obtained by electrolysis . Floating agents specifically have included hostaflon powder, aluminum particles, confetti, pellets and textile filaments.

3-7 The Rotating Cube Technique

This technique has been first reported by Seddon and Anwar(1963), and then used by Anwar(1965,1967,1969), to measure different velocity components. The technique in principle requires minute particles suspended in the water to be visualised. They are illuminated in a narrow light beam, and observed by telescope through a rotating glass cube with optically ground faces. They appear to be stationary when the cube is rotated at a speed related to their actual speed, calibration of the apparatus being necessary. Anwar reported that it was possible to measure velocities of up to 3m/sec, and with suitable orientation of the axis of rotation velocity components at other inclinations could also be measured.

3-8 Laser-Doppler Anemometry

Laser Doppler Anemometer is an optical technique which utilises the transit time of small solid particles across a known number of interference fringes generated by two light beams, in order to

measure a velocity component. Fig.(3-8-1) shows the interference pattern produced by two mutually coherent light beams which could for example, have originated from points on the same wave front. This interference pattern changes position as the two beam sources move, producing intensity variations . Laser Doppler Anemometry uses an extension of this principle in that the corresponding physical processes can be completely described in term of interfermometry and by the displacement of the interference patterns caused by movements of scattering particles. Photodetectors are employed to detect these intensity variations and result in electrical signals with frequency related to the velocity of a particle, its position relative to the light sources and photodetector, and the frequency of the sources.

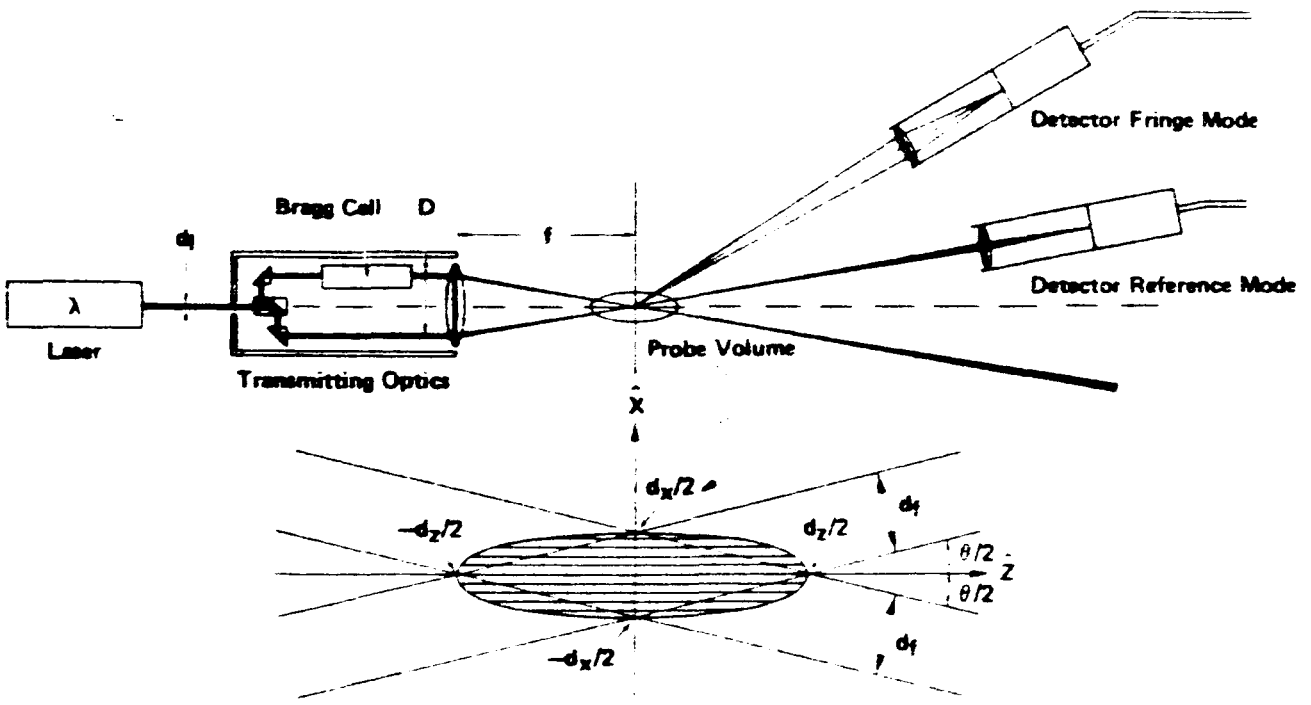

Fig. 3-8-1 Interference Pattern Produced by Two mutually Coherent Light Beams

The interference pattern may be real or virtual, depending upon whether incident beams are crossed or scattered . Whichever mode is used, a Laser Doppler Anemometer system comprises a light source (which is always a Laser) , optical arrangements to transmit and collect light, a photodetector and a signal processing arrangement.

The laser is a source of coherent light of appropriate intensity, its beam may be split into two parts which cross to provide an interference pattern in the local region of the flow where velocity measurements are required. Part of the volume of interference is observed by a light collecting system and focussed on a photodetector. The photodetector converts the optical signal to voltage, which is then filtered and processed electronically. Laser Doppler Anemometer could be used for:

1-Measurement of a rate of flow,the anemometer being used to measure local instantaneous velocity which can be related to volumeteric-flow rate by integrating a measured velocity profile or by knowing the profile shape.

2-Velocity and velocity change, the rapid response to velocity change which is available in Laser Doppler Anemometers can also be of value to flow measurement applications. The accurate measurement of velocity itself has led to its utilization in the calibration of Total-Head Props, and to its measurements of wind speed

at long distance (Durst etal. 1981). The sensitivity to changes in velocity helps in sensing unexpected surges in gas mains or in mines.

3-Measurements of instantaneous velocity and its correlation, Laser Doppler Anemometer is capable of measuring the instantaneous velocity and its correlation which is of great help in evaluating some of the unresolved quantities in the turbulent models.

CHAPTER FOUR

MATHEMATICAL FORMULATION

4-1 Introduction

Analysis of the flow regime in the vicinity of a vortex has been stated by all previous workers to be complex, and incapable of absolute solution. They proposed solutions in which the mathematical complexities were alleviated by making simplifying assumptions. It was recognised that one universal set of equations was inappropriate to describe the various flow fields, and suggestions to identify the locations of the different types of flow made.

The present investigation method enabled velocity measurements, together with their fluctuations to be obtained through many of these individual flow fields. A method of analysis is shown which enabled the Reynolds Shear Stress $(\overline{u'v'})$ and the eddy viscosity (ε) to be evaluated within close proximity of the outlet, and also to determine the areas within which their effects are significant.

LEWELLEN (1962) divided the vortex flow in a confined vortex tube into three regions fig.(4-1-1). these regions were:

a- Region I ; $R \geq r \geq ro$, $L \geq z \geq \delta$

b- Region II ; $R \geq r \geq ro$, $\delta \geq z \geq 0.0$

c- Region III; $ro \geq r \geq 0.0$, $L \geq z \geq 0.0$

where r is the radial distance, z is the axial distance, R is the radius of the vortex tube, ro is the outlet radius, δ is the boundary layer thickness and L is the length of the vortex chamber.

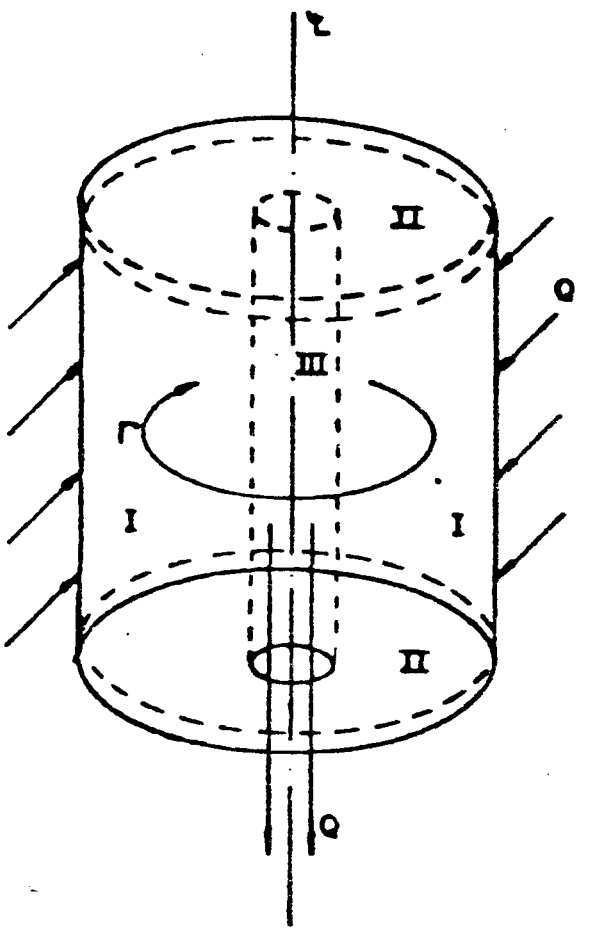

Fig.4-1-1 Flow regions in a cylindrical confined Vortex chamber (after Lewellen, 1962)

LEWELLEN (1976) divided the vortex flow over a solid surface (as in the case of a tornado) into four regions, as shown in fig.(4-1-2). In region I similarity solutions may be considered. In region II boundary layer flow can be assumed. Region III is the

most complex one, the complete set of Navier Stokes Equations without similarity assumptions and with the inclusion of turbulence terms must be solved. Region IV depends strongly on the total vortex flow.

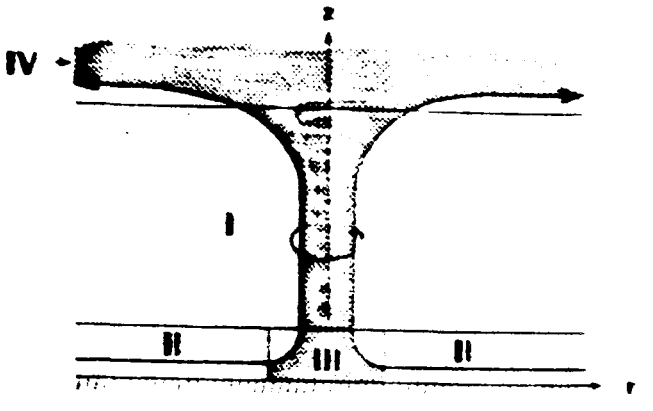

Fig. 4-1-2 The four regions of vortex flow over a flat surface, exemplified by a tornedo

(after Lewellen 1976)

In reality, as in the case of a tornado, strong interactions with the adjacent enviromental weather situation occur, which to a large extent maintain the vortex. All regions interact with each other, and adjustments at their borders must be made. Perturbation techniques, which facilitate the matching, are recorded by ROTT and LEWELLEN (1966), GRANGER (1966) and VAN DYKE (1964).

4-2 Shear Stress Conventions

In a 2-dimensional system, the assumption is that velocities u and v increase in the directions x & y fig(4-2-1a). Shear

stresses $\tau_{xy} = \tau_{yx}$ will act on the advancing face of the element in the directions x & y, because the velocities u and v increase in those directions.

From the fundamental Navier Stokes equations, the components of the stress tensor in the x-direction due to turbulence are:

4-2-1 $$(\tau_{xx} \; \tau_{xy} \; \tau_{xz}) = -\rho \left(\overline{u'^2} \;\; \overline{u'v'} \;\; \overline{u'w'} \right)$$

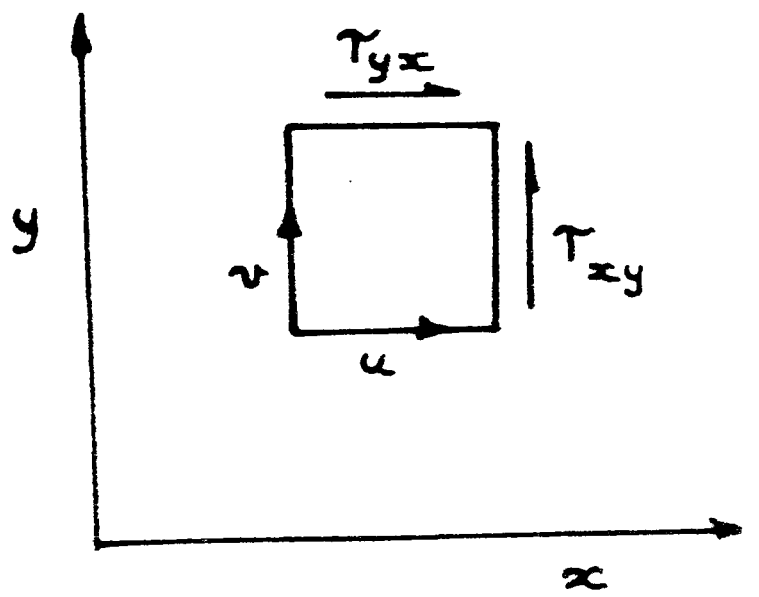

Fig. 4-2-1a Directional Conventions

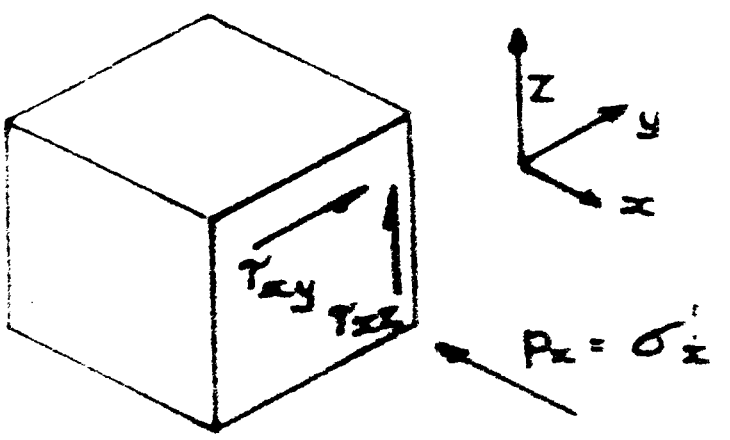

Fig. 4-2-1b Force System acting on the Face of a Unit Cube

with x,y,z,u,vand w all increasing togther, then the force system acting on the face of a unit cube is as shown in fig (4-2-1b) δ'_x clearly acts in negative x, and hence; $\delta'_x = -\overline{\rho u'^2}$ is correct, u'^2 cannot be negative, therefore the argument is justified.

The shear stress τ_{xy} in a similar system, clearly acts in the direction shown and is derived as $\tau_{xy} = -\overline{\rho u'v'}$, τ is positive, hence $\overline{u'v'}$ must be a negative quantity.

4-3 Basic Theoretical Equations

The starting point for any mathematical treatment of the flow of an incompressible viscous fluid is the Navier-Stokes equations which are, in vector form:

$$DV/DT = F - (1/\rho)\Delta P - \nu\nabla\Lambda(\nabla\Lambda V) \qquad 4\text{-}3\text{-}1$$

where F is an external body force per unit mass acting on the fluid (e.g. where the Coriolis forces is important, MARRIS (1967))

$$F = -2\,\Omega\Lambda V \qquad 4\text{-}3\text{-}2$$

The Navier-Stokes equation is an application of Newton's second law to a fluid and hence is sometimes called the momentum equation. Another equation which is necessary is the continuity equation:

$$\text{div } V = 0 \qquad 4\text{-}3\text{-}3$$

for incompressible flow with no sources or sinks.

For the geometrical configurations considered in this research work, the obvious co-ordinate system is cylindrical polar co-ordinates, hence equations 4-3-1 and 4-3-3 become, in component form:

a- Radial component

$$4\text{-}3\text{-}4 \quad D'u/Dt - v^2/r = -(1/\rho)\,\partial p/\partial\theta + \nu(\,\nabla^2 u - u/r^2 - (2/r^2)(\partial v/\partial\theta))$$

b- Tangential component

$$4\text{-}3\text{-}5 \quad D'v/Dt + uv/r = -(1/\rho)\partial p/\partial\theta + \nu(\nabla^2 v + (2/r^2)\partial u/\partial\theta - v/r^2)$$

c- Axial component

$$4\text{-}3\text{-}6 \quad D'w/Dt = -\,(1/\rho)\partial P/\partial z + \nu(\,\nabla^2 w)$$

The two operators D'/Dt and ∇^2 are:

$$4\text{-}3\text{-}7 \quad D'/Dt = \partial/\partial t + u\,\partial/\partial r + (v/r)\partial/\partial\theta + w\,\partial/\partial z$$

and

$$4\text{-}3\text{-}8 \quad \nabla^2 = \partial^2/\partial r^2 + (1/r)(\,\partial/\partial r) + (1/r^2)(\partial^2/\partial\theta^2) + \partial^2/\partial z^2$$

For a steady axially symmetrical flow about the vertical axis of a cylindrical tank $\partial/\partial t = 0$ and $\partial/\partial\theta = 0$ thus, equations 4-3-3,4 and 6 reduce to the following:

a- Radial component

4-3-9 $$u\partial u/\partial r + w\partial u/\partial z - v^2/r = -(1/\rho)\ \partial p/\partial r + \nu(\partial^2 u/\partial r^2 + 1/r\ \partial u/\partial r + \partial^2 u/\partial z^2 - u/r^2)$$

b- Tangential component

4-3-10 $$u\partial v/\partial r + w\partial v/\partial z + uv/r = \nu(\partial^2 v/\partial r^2 + 1/r\ \partial v/\partial r + \partial^2 v/\partial z^2 - v/r^2)$$

c- Axial component

4-3-11 $$u\partial w/\partial r + w\partial w/\partial z = -(1/\rho)\ \partial p/\partial z + \nu(\partial^2 w/\partial r^2 + 1/r\ \partial w/\partial r + \partial^2 w/\partial z^2)$$

and the continuity equation

4-3-12 $$1/r\ \partial(ur)/\partial r + \partial w/\partial z = 0$$

Equations 4-3-9,10 and 11 are applicable to steady flows in which the instantaneous point velocities are the same as the time averaged velocity

$$u = \overline{u}$$

4-3-13 $$v = \overline{v}$$

$$w = \overline{w} \qquad \text{and } p = \overline{p}$$

i.e. Laminar flow.

For turbulent flows the instantaneous velocity varies with time , and is different from the mean

$$u = \overline{u} + u'$$

4-3-14 $$v = \overline{v} + v'$$

$$w = \overline{w} + w' \quad \text{and } p = \overline{p} + p'$$

(where the bar signifies average whilst (') represents the fluctuation which has a zero time average). Equations 4-3-10,11 and 12 will be rewritten in their turbulent form with the following assumptions:

1- The time average of the fluctuation will be zero (i.e. $u' = v' = w' = p' = 0$)

2- The first and second derivitives of the time average of the fluctuation will also be zero .

3- The effective viscosity is equal to $\nu+\varepsilon$ (where ε is the eddy viscosity).

For simplicity and where no possibility of confusion can arise, the bar signifying average velocity will be now omitted.

a- Radial component

4-3-15 $$u\partial u/\partial r + w\partial u/\partial z - v^2/r - v'^2/r = -1/\rho\ \partial p/\partial r + (\nu+\varepsilon)(\partial u^2/\partial r^2 + 1/r\ \partial u/\partial r + \partial^2 u/\partial z^2 - u/r^2)$$

b- Tangential component

4-3-16 $$u\partial v/\partial r + w\partial v/\partial z + uv/r + u'v'/r = (\nu+\varepsilon)(\partial^2 v/\partial r^2 + 1/r\ \partial v/\partial r + \partial^2 v/\partial z^2 - v/r^2 + u'\partial v'/\partial r + w'\partial v'/\partial z)$$

c- Axial component

4-3-17 $$u\partial w/\partial r + w\partial w/\partial z = -1/\rho\ \partial p/\partial z + (\nu+\varepsilon)(\partial^2 w/\partial r^2 + 1/r\ \partial w/\partial r + \partial^2 w/\partial z^2)$$

and the continuity equation

4-3-18 $$1/r\ \partial(ur)/\partial r + \partial w/\partial z + 1/r\ \partial(ru')/\partial r + \partial w'/\partial z = 0$$

Under the previous assumptions the first two terms of equation 4-3-18 alone are equal to zero, since the flow is steady. Therefore, the sum of the last two terms must also be zero at every instant, not only as an average. If this sum of the last two terms is multiplied by v', then equation 4-3-18 could be split into two parts

4-3-19a $$1/r\ \partial(ru)/\partial r + \partial w'/\partial z = 0$$

4-3-19b $$v'/r\ \partial(ru')/\partial r + v'\partial w'/\partial z = 0$$

or

4-3-20 $$v'\partial u'/\partial r + u'v'/r + v'\partial w'/\partial z = 0$$

Subtracting equation 4-3-20 from the fluctuation terms of equation 4-3-16 and applying the assumptions above, equation 4-3-16 takes the following form;

$$4\text{-}3\text{-}21 \qquad \partial\overline{u'v'}/\partial r + 2\overline{u'v'}/r + \partial\overline{v'w'}/\partial z =$$

$$(\nu+\varepsilon)(\partial^2 v/\partial r^2 + 1/r\ \partial v/\partial r + \partial^2 v/\partial z^2 - v/r^2)$$

$$-(u'\partial v'/\partial r + w'\partial v'/\partial z + uv/r)$$

Equations 4-3-15,17 and 21 are Reynolds equations for radial, axial and tangential components under the assumptions made.

4-4 Flow Regions

Based on the descriptions suggested by Lewellen (1976), the data derived from this work enabled the flow in an unconfined free surface vortex to be designated as follows.(Fig. 4-4-1):

1- Region I : a thin layer in contact with base and side wall within which boundary layer forces predominate. This is conveniently referenced as a region of Base Flow. This was not investigated in any detail.

2- Region II : the bulk of the volume of fluid contained within the cylinder, in which the radial and axial components tend to zero (i.e. $r \geq r^{\bullet}$; $z \geq z^{\bullet}$). The predominant motion is rotational, and the region is hence designated as one of Tangential Flow.

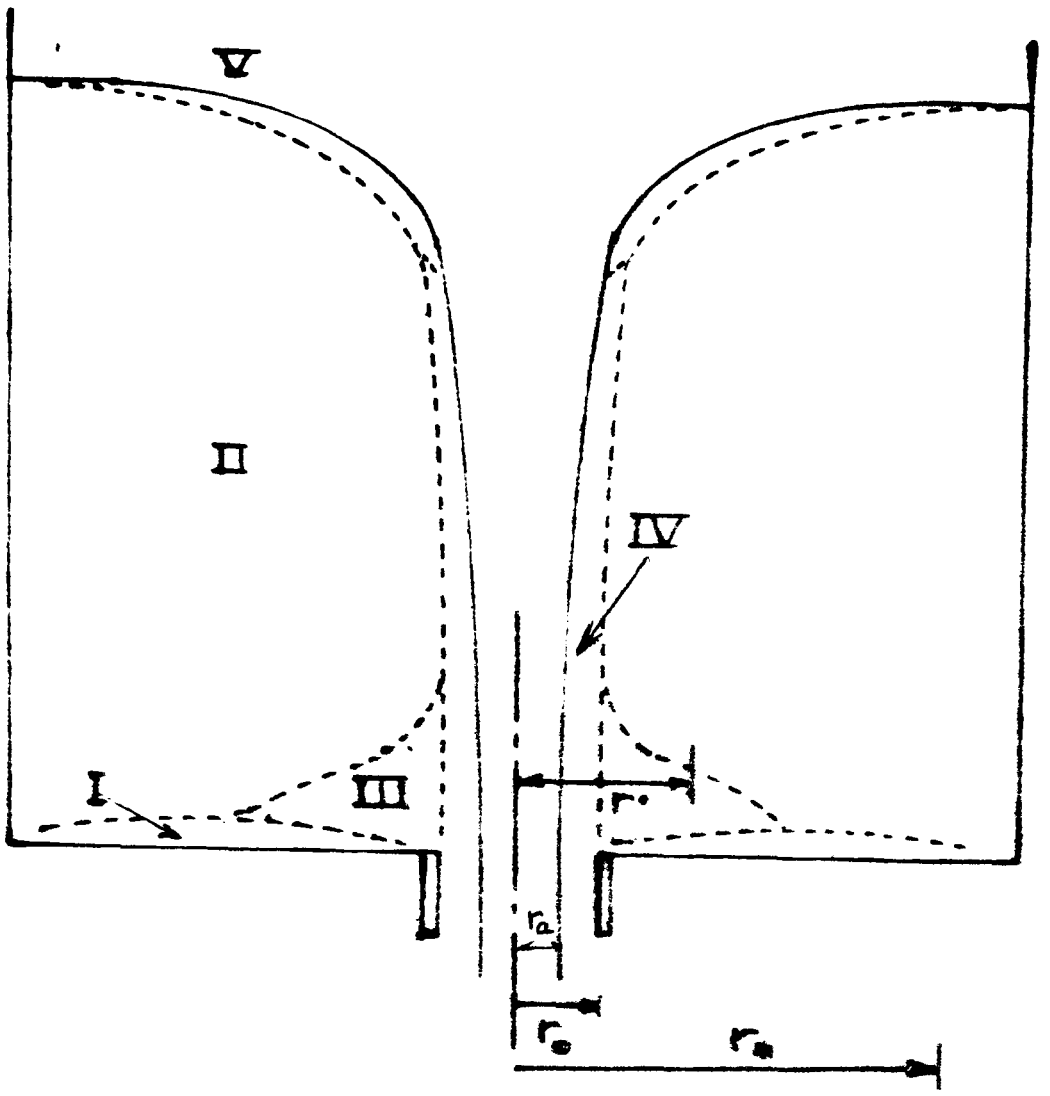

Fig. 4-4-1 Proposed Flow Regions in an unconfined Vortex

3- Region III : a confined area between the Base and Tangential Flow zones and adjacent to the outlet within which the increasing tangential velocity of Region II is retarded by the influence of the boundary layer forces on the base, and centripetal accelerations towards the outlet generated. Within this region, the fluid particles acquire an increasing radial velocity, so a zone of Accelerating

Flow is an appropriate term. The limits are imprecise, but generally $r^{\bullet} \geq r \geq ro$ and $z^{\bullet} \geq z \geq \delta$.

4- Region IV : a cylindical volume with $r \leq ro$ and bounded by the central air core. Very rapid velocity gradients influenced by the drag effects of the air/water interface occur, but were not investigated. Core Flow appears to describe these characteristics.

5- Region V : the upper layer of Region II, comprising the air/water interface and its environs. The region can be described as one of Surface Flow, and was incapable of meaningful investigation.

4-4-1 Base Flow region (I)

The tangential velocity component only differed from the velocity in Region II at small radii, but measurements made in the appropriate areas were unreliable with the rig used, due to the laser light reflected from the various interfaces producing better signals than those from the measuring volume. Axial velocity measurements nearer than 20mm from the base were beyond the capability of the optical system.

4-4-2 Tangential Flow region (II)

In this region the following assumptions could be made:

$u = 0$, $w = 0$, p = constant. $\partial^2 v/\partial z^2 = 0$, $\varepsilon = 0$, and $\overline{u'v'} = 0$

. From which equation 4-3-21 becomes :

4-4-1 $$v = r^{\bullet 2}(\partial^2 v/\partial r^2 + 1/r^{\bullet}\ \partial v/\partial r)$$

Values of $r^{\bullet}$ which satisfy equation 4-4-1 will mark the end of Region (III) and the beginning of Region(II). Experimental data provides the relationship of $v = f(r)$ and hence equation 4-4-1 can be solved.

4-4-3 Accelerating Flow region (III)

This is the most complex region in an unconfined vortex flow, since it is a region of transition between regions I ,II and IV. A mathematical model of this region based on equations 4-3-15,17 and 21 is proposed, making the following assumptions:

a- The term $\partial\overline{v'w'}/\partial z$ will be assumed to be zero, since the axial velocity component is small compared with the radial and tangential components.

b- By analogy with laminar flow in a curved path, the following expression can be written for the Reynolds shear stress in turbulent flow (Anwar 1969)

4-4-2 $$\tau_{uv} = -\ \rho\overline{u'v'} = -\ \rho\varepsilon(\partial v/\partial r - v/r\ )$$

let

$$\partial^2 v/\partial r^2 + 1/r\ \partial v/\partial r - v/r^2 = F1$$

$$u\partial v/\partial r + w\partial v/\partial z + uv/r = F2$$

and

$$\partial v/\partial r - v/r = F3$$

then substituting the value of $\overline{u'v'}$ from equation 4-4-2 above into equation 4-3-21, one gets

4-4-3 $$\partial/\partial r(\varepsilon F3) + 2\varepsilon F3/r = \nu F1 + \varepsilon F1 - F2$$

The left hand side of equation 4-4-3 is

$$\varepsilon \partial/\partial r(\partial v/\partial r - v/r) + F3\ \partial\varepsilon/\partial r + 2\varepsilon/r(\partial v/\partial r - v/r)$$

which on further expansion becomes $\varepsilon\ \partial^2 v/\partial r^2 - \varepsilon/r\ \partial v/\partial r + \varepsilon v/r^2 + 2\varepsilon/r\ \partial v/\partial r - 2\varepsilon v/r^2 + F3\partial\varepsilon/\partial r$

Hence equation 4-4-3 becomes

$$\varepsilon\ F1 + \partial\varepsilon/\partial r\ F3 = \nu\ F1 + \varepsilon\ F1 + F2$$

or

4-4-4 $$\partial\varepsilon/\partial r = (\nu\ F1 + F2)/ F3 = F4$$

Equation 4-4-4 can be solved for ε if F4 is a function of r. From which

4-4-5 $$\varepsilon = \int F4\ dr + C$$

with the boundary condition $\varepsilon = 0$ at $r \geq r_\bullet$ then

4-4-6 $\quad C = \int F4\ dr \quad$ when $r = r_{\bullet}$

The value of $\overline{u'v'}$ can then be found by substituting the value of ε obtained from equation 4-4-5 into equation 4-4-2. These values will be discussed in the following chapters.

CHAPTER FIVE

EXPERIMENTAL WORK

5-1 Introduction

This chapter includes details of the first and second models used in this research work, the procedure followed in collecting the data , determination of the geometric centre and of the centre of rotation. It is worth mentioning that each run took about six hours to complete because the Laser Doppler Anemometer incorporated was of the one component model (i.e. it was possible to measure one velocity component with it's RMS (Root Mean Square) at each setting. The total number of velocity measurements made and analyzed was about 20000.

5-2 First Model

A rectangular channel 500mm wide and 300mm deep was fabricated in perspex type material. A flanged outlet permitting vertical pipes with diameters up to 75mm was fitted into the base ,and the depth of flow controlled by a weir at the downstream end. This channel of 4.6m length was directly attached to a large header tank containing baffles and fed from the laboratory ring main.

The Laser Doppler Anemometer was mounted on the bed of a milling machine, enabled movement of the laser to be made and measured accurately in three mutually perpendicular directions. The air

core formed at the heart of the vortex which developed above the outlet pipe precluded the use of the Laser in forward scatter mode, with the photomultipier sited behind the vortex. A back scatter mode, was used, the photomultipier being sited on the transmission optics itself. Due to the physical magnitude of the this model, and the length of the laser paths, the amount of signal received back was very small, and was often submerged within the electronic noise. Whilst some data were obtained to enable velocity profiles adjacent to the vortex to be drawn, it was considered that the quality and accuracy of these measurements was suspect and could not be guaranteed.

These short comings in the method of investigation are regrettable, but are to some extent the result of dubious advice regarding laser power requirements given by the manufacturers.

In spite of the unsuitability of the apparatus to measure accurately using the back scatter mode, it became clear that its capabilities in the forward scatter mode would enable the investigation to proceed, providing the air/water interface was avoided. Using this arrangement, designed to apply few restrictions to the vortex formation, it had soon become apparent that very slight disturbances in the flow conditions within the channel caused the air core to deviate, making determination of the centre of rotation virtually impossible. Introduction of

guide vanes around the outlet stabilized conditions, but proved to be too restrictive on lines of sight for the laser gun.

It was decided to use this model as a means of establishing the capability of the Laser Doppler anemometer and it's sensitivity to velocity fluctuations and a computer program (BASIC) was developed to enable communications and transformations of the data between the Tracker and a microcomputer (PET32K)to be made.

The experimental work carried out on this model, established some flow patterns in a rectilinear flow with a sink, the results of this investigation not being included in this research work.

5-3 Second Model

Incorporating the experience gained in operating the first model an open topped cylindrical tank 600mm diameter and 330mm in height with a symmetrically placed outlet with a flange fitting capable of accepting pipes up to 100mm, was constructed. Careful fabrication, with lips or other protrusions likely to disturb flow towards the outlet pipe which itself was also square ended, were eliminated. In order to minimize some of the inherent difficulties in making optical measurements through a curved surface, the cylindrical tank was contained within a slightly larger rectangular chamber, the water depths being equalized. This system had the advantage of permitting the vertical wall of the cylinder to be of thin perspex (2mm), reducing the refraction and translation of the laser beams.

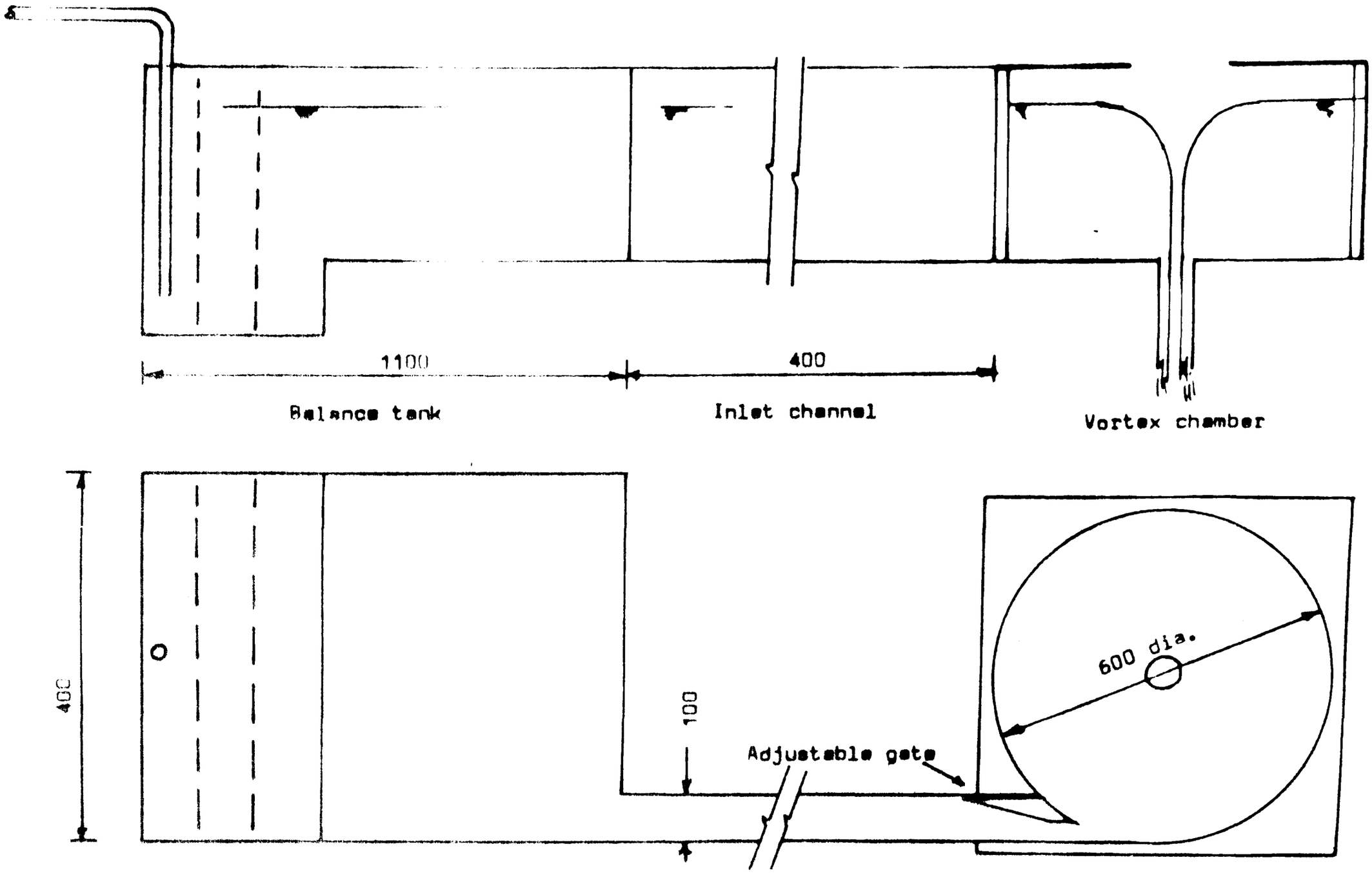

FIG. 5-3-1 General Arrangement of the Apparatus

Water was supplied to the model by recirculating pump from the laboratory sump, frequent changes being necessary due to the formation of algae deposits causing turbidity and hence loss of laser signal quality. The vortex chamber (i.e. the cylindrical tank) was supplied with water from a channel connected to a stilling tank, the outer wall being tangential to the vortex chamber. Variation in entry velocity was controlled by changing the width of the channel and this was achieved by the insertion of shaped reduction pieces. The widths of opening so achieved were 27,55, and 100mm, the apparatus being generally as shown in Fig(5-3-1).

Flow rates were measured by timed collection in a calibrated tank below the outlet.

5-4 Laser Doppler Anemometer

5-4-1 Introduction

The anemometer combines optical and electronic systems which when correctly adjusted enables the velocity of discrete particles moving with the fluid to be measured. The sensing agency is a system of light beams which pass through the fluid to intersect at the point of interest, light reflected by moving particles at that location transmitting the information back to an electronic analysing device. No physical obstruction is introduced into the fluid, and hence the flow pattern is undisturbed, the magnitude of the velocity and direction of the fluid motion at the gauging point being totally unaffected. Such a system clearly has great

advantages over others involving the introduction of current meters and pitot tubes. Use of such apparatus in the rapidly rotating core of a free vortex would be impossible, and it is recognised that this investigation would have been impossible without the use of the Laser Doppler Anemometer.

5-4-2 Optical System

It is well known that at the intersection of two light beams polarised in the same plane, a fringe system consisting of alternate light and dark bands is created, oriented to bisect the angle between the beams. Solid particles crossing the fringes will reflect bursts of light at a frequency related to the frequency of the light beams and the velocity of the particles. At low speeds, where the mean velocity differs only slightly from zero , the instantaneous velocity fluctuations can clearly be in the general direction of motion or oppose it, and the frequency of the reflected light not be representative of the particle velocity. However if the frequency of the wave characteristic of one incident beam is changed, then the fringes generated in the measuring volume will move across the line of the beams. By so doing, the signals representing the mean velocity and the fluctuations can be made to be wholly of the same sign, and the direction of the flow velocity determined.

The light source is a single low powered laser, which is split as it passes through a glass prism, and one separated beam passes

through an acousto-optical frequency shift cell, which changes the wavelength of the laser light, and hence the frequency of its wave form. The two beams are then fed into a conventional optical system, which separates them to a variable spacing in the range 13 to 39mm, before focussing them at the measuring volume.

The optical design ensures that the lengths of travel of each beam within the optical system are equal, by introducing a compensating glass rode in the Bragg Cell.

5-4-3 Electronic System

The system requires that the bursts of light emitted as a particle crosses the fringes is collected by a lens system and focussed on a photo-electric cell, where a current is generated and sent to the Tracker unit. The device is known as a Photomultiplier, which requires careful adjustment to ensure that the maximum amount of light emitted from the measuring volume is concentrated on the photo-sensitive cell. This signal is analysed by the Tracker unit, the current magnitude being converted to a frequency, and subtracted from the frequency of the moving system in the measuring volume. Suitable filters and electronic frequency shift are incorporated so that the correct Doppler frequency is read, and errors of one or more wave lengths avoided. The controls enabling the optical frequency shift of ±40MHZ to be made, and the electronic range and sensitivity of the Tracker are available, together with visual indications of signal quality and strength.

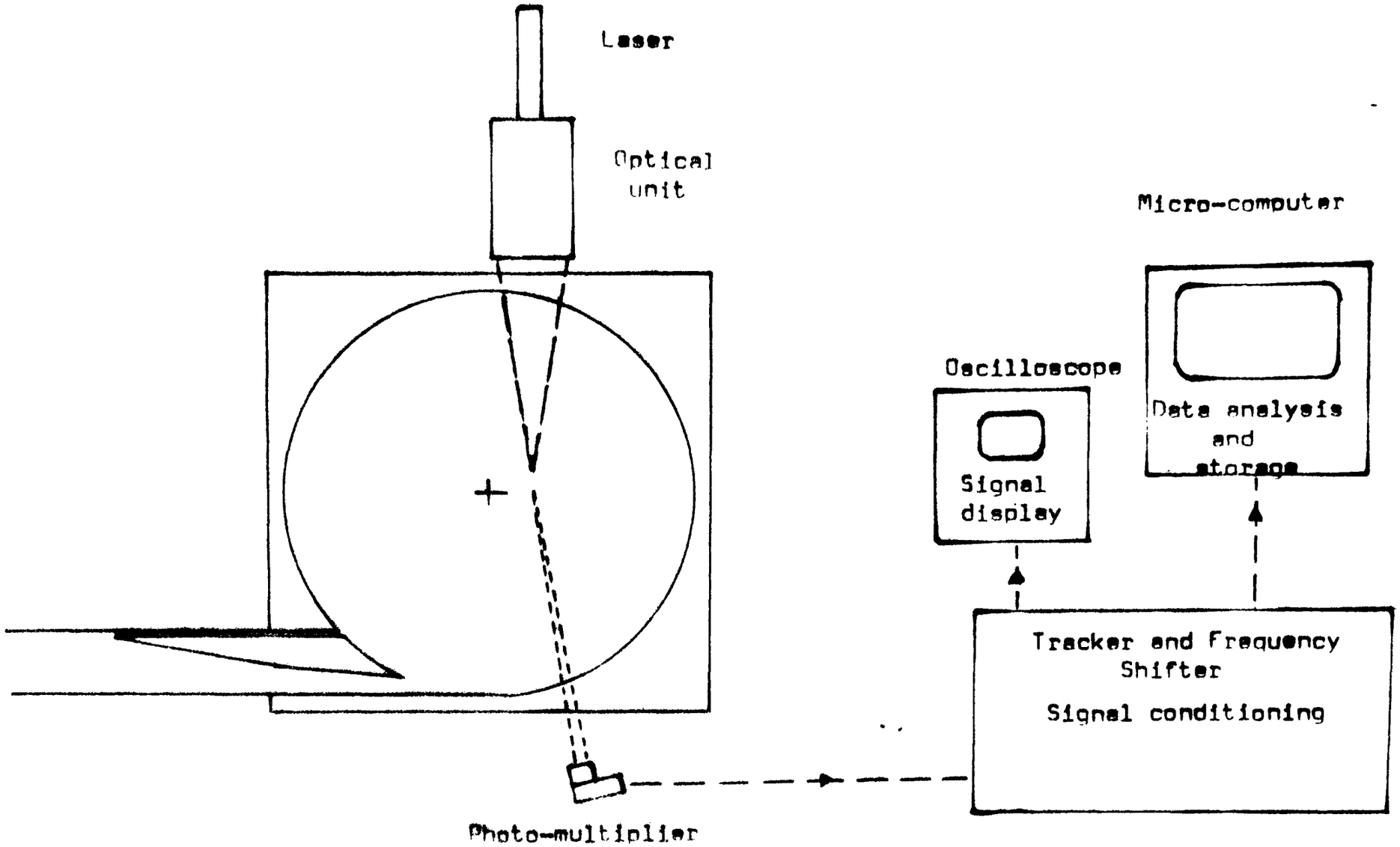

FIG. 5-3-2 General Arrangement of the Apparatus

In addition an oscilloscope was permanently connected on which the envelope of the signal to be analysed was constantly displayed.

5-4-4 Method of Use

In this work, where, adjacent to the air core a large change in velocity was expected for a very small change in radius, it was essential to be able easily to relate the position of the measuring volume to a known point. The obvious reference point is the centre of the outlet pipe, and this was located by moving the beam intersection to a steel pin placed in the centre of the outlet pipe. Whilst this was done, the cylindrical tank and surrounding chamber were full of water. This location was referenced back to the milling machine bed, on which the laser and the optical system was mounted.

By operation of the feed screws controlling the movement of the milling machine bed, the measuring volume was located where a velocity was to be measured and its three dimensional co-ordinates recorded. The Photomultiplier was set slightly off-line from the laser lights, and its focussing screws adjusted until the received light entered the pin hole in a small screen, as seen through a microscope. When this adjustments had been satisfactorily made, reflections and refractions from other sources were known to be precluded, and hence the best quality of signal was being sent to the Tracker. It was found that the signal quality and strength as indicated by the Oscilloscope was a reliable guide. The signal

sent from the photomultiplier depends on its supply voltage, which to reduce electronic noise needs to be kept to a minimum, otherwise the required signal at the Tracker becomes submerged. This voltage adjustment was made within these limiting criteria. The frequency of the signal from the photomultiplier will differ from ± 40MHZ by an amount due to the particle velocity, and so the Tracker must be set with a range across ±40MHZ sufficient to encompass the particle velocity and its fluctuations. The ±40MHZ frequency is already set with the Tracker unit, and the range of frequencies to which the system is sensitive is set with external controls.

By making the Tracker operate at the widest range of frequencies, then the mean velocity can be measured, but the fluctuations will not generate sufficient variations to be noteworthly. It is essential that the correct range of frequency variation is chosen, and much care was taken to achieve this.

When signals of satisfactory quality and strength were being received, the program in the microcomputer was started and data collection commenced. The Tracker unit itself discarded some extreme values because of the design of the output port, but all other readings were sent directly into the memory storage area of the microcomputer. The rate of transmission was 60 bytes per second, and generally data were collected over a 10 seconds period. This period of 10 seconds was chosen after the photographs (plates 5-4-1 and 2) showed that the air core location and stability was

maintained for at least that period of time. The program then processed the data to provide values for mean velocity and its fluctuation as the RMS value.

5-5 Centre of Rotation

In order to define the centre of rotation a detailed analysis of the flow pattern was needed specially in the area close to the air core. Velocity measurements VL were taken on a rectangular grid of 5mm radially and 2mm along the line of the Laser beam. The origin for referencing this series of measurements was the geometric centre along the laser beam, and the centre of the air core perpendicular to it, as ascertained by contact of the laser beam with the air/water interface, at both sides. It was found that reliable measurements could be obtained no nearer than 6mm to the base, and consequently the analysis was carried out there and 10mm and 5mm intervals of height thereafter. Three flow rates were used keeping the outlet pipe diameter and inlet velocity constant. The convention adopted was to consider the velocity component positive when towards the air core, and negative when away, and the data as recorded after analysis by Doppler shift method is plotted in Figs. 5-5-1 to 5-5-24 . These plots show the velocity profiles of VL for a distance ± 21mm along the laser beam, with the origin at the geometrical centre of the outlet. The profiles are at 5mm intervals between 15 and 40mm from the centre of the air core measured perpendicular to the laser in a horizontal plane.

The data was analysed by the mainframe computer, and lines of best fit drawn at equal values of VL. Statistical methods and successive iterations were applied to locate a centre point about which the fluid was rotating. For the analysis to be valid, then one test should include this procedure to find the centre point, immediately followed by the measurements of data required in the overall project. This was more than one days' work, and the process was not applied, it being considered unlikely that identical conditions could be achieved next day.

An alternative method was developed to determine the centre of rotation approximately, making use of the change in the axial velocity as a guide. The laser optics were rotated 90 degrees so as to be sensitive to the axial velocity component, and the measuring volume moved in and out alongside the air core and close to it. By observing the changes in the instantaneous velocity, the centre of rotation was assumed to occur at the same co-ordinate as the maximum reading obtained. The location of the centre of rotation was found at each level by the same method as described above. Because the optical system used needed to be of long focal length, measurements of axial velocities less than 20mm above the base could not be made, so the velocity at that level was also assumed for lower points.

5-6 Velocity Measurements

The programme of work required velocities and fluctuations of velocities to be measured at locations throughout the whole of the flow region and this system was found to be capable of the measurement of velocities and fluctuations in radial, axial and tangential directions. In operation, the motion of the laser was indexed from the centre of rotation estimated for a particular level, and the radial and axial velocities measured at radii along the diameter perpendicular to the laser beam. By feeding relevant co-ordinates into the microcomputer, the co-ordinates of another point on the same radius (as near as possible to the air core) but at some angle θ from the perpendicular diameter were determined, and the measuring volume relocated to measure the velocity component there. Axial and radial velocity components and their fluctuations were measured directly, whilst the tangential velocity component and its fluctuation were calculated.

This procedure was repeated at different geometries, utilizing, outlets of three different sizes (28 , 38 , 53mm in diameter), three different entry widths (27 , 55 , 100mm), and varying flow rates, producing about 20,000 data items each generally resulting from a sample size of 600 readings.75% of the above procedure was repeated for second checking and the results obtained were found to be in close agreement with the first estimates. In addition spot

checks of the mean velocity measurements were carried out at different times and good agreement found.

Plate 5-4-1 Air Core

Single instantaneous Exposure

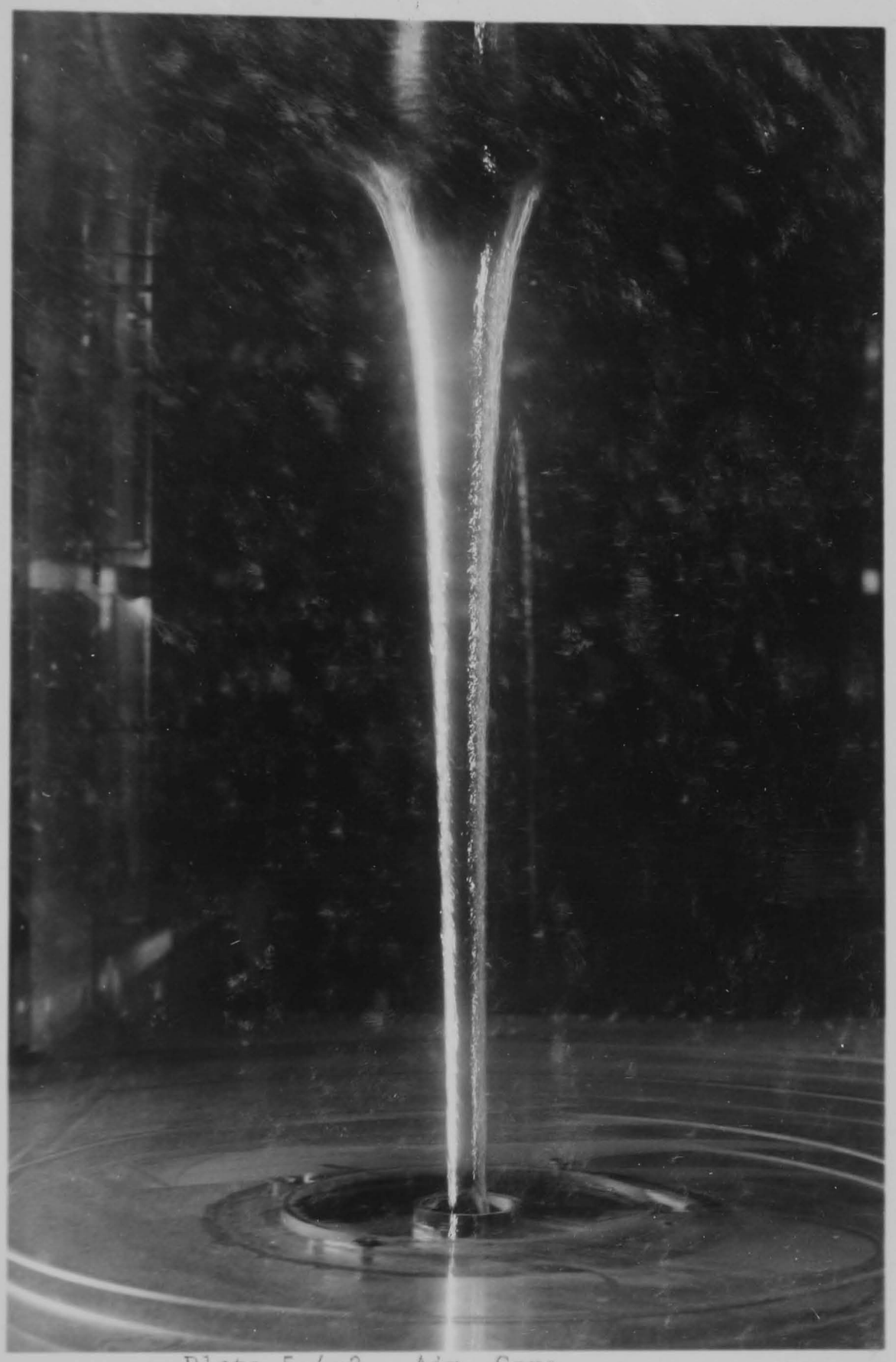

Plate 5-4-2 Air Core

Thirteen Superimposed Exposures within period of ten seconds

CHAPTER SIX

RESULTS AND DATA ANALYSIS

6-1 Introduction

This chapter describes the flow properties in a vortex chamber based on the experimental data. Description of the results includes the process followed in the analysis of the experimental data, and the physical interpretation of the profiles obtained. Results are described in the following sequence:

6-2 Flow properties determined by measured velocity components.

6-3 Dimensional analysis

6-4 Average velocity components(u,v,w)

6-5 Velocity fluctuations (u',v',w')

6-6 Shear stress ($\overline{u'v'}$) and eddy viscosity (ε).

6-7 Flow boundaries

6-8 Geometrical proportions

Because of the excessive amount of time that would have been needed to make detailed mean and fluctuating velocity measurements in an entire cross-section of the vortex chamber, measurements for the determination of the centre of rotation were carried out in two quadrants of the chamber whilst all other measurements were made in one quadrant only. Only the first and the second quadrants

where accessible by the laser due to the physical configuration of the vortex chamber.

6-2 Flow properties

The flow properties were investigated by measuring the three velocity components, the radial and tangential components in the horizontal plane, and the axial in the vertical plane.

Figures 6-2-1 to 6-2-6, show that generally throughout the vortex, the axial velocity component is very small, and near the outlet, it is relatively insignificant as compared with the radial and tangential velocities.

Figures 6-2-7 to 29 show the profiles of the radial and tangential velocity components. The shape of these indicates that there are clearly defined boundaries between the different flow regions, approximating to the demarcations suggested in the theoretical analysis formulated in Chapter Four. The boundary limits of each of these regions will be discussed in section 6-7.

6-3 Dimensional Analysis

The principle of dimensional homogeneity as an aid to the design of experimental procedures, and as a method of analysing data resulting from experiments is a well tried technique.

Conventionally two dimensionless groupings formed from the data are plotted, all others being held constant, the process being repeated for all non-dimensional groups. By this means the applicability or otherwise of these groups becomes apparent. By com-

bination of multiples and powers of some non-dimensional groups, all the data can be made to consolidate onto plots which are clearly similar but differ according to the groups held constant.

In order to take advantage of the principle without the necessity of controlling the individual groups, the method of compounding (Sharp 1981) was used. A computer program to evaluate the relative constants and indices in order to relate the experimental data was developed.

The following dimensionless combinations were formed:

6-3-1 v/V ,r/R,z/R,b/R,ro/R,h/R,VR/ν,$V/\sqrt{gR}$

It is postulated that the velocity profile at outlet is completly different from that at inlet, flow changing from laminar to turbulent. One possible criterion to distinguish the location of the change point is the point at which fluctuations in the tangential velocity become significant. This appears to occur at differing radii for different heights above the base.

For the Tangential Flow region (II) , the velocity v_2 at radius r and height z is the relevant tangential velocity component parameter , conditions being dependent on the inlet and outlet conditions.

The suggested groupings for this region then become

6-3-2 v_2/v_*, r/r_*, z/r_*, b/r_*, ro/r_*, h/r_*, v_*r_*/ν, $v_*/\sqrt{gr_*}$

Considering the zone of Accelerating Flow (III), in which from figures 6-2-7 to 6-2-29 it can be seen that radial accelerations are important, the upstream boundary condition is v_2. Hence the possible dimensionless groupings of the basic parameters become

6-3-3 v_3/v_2, $r/r^\bullet$, $z/r^\bullet$, $ro/r^\bullet$, $h/r^\bullet$, $v_2r^\bullet/\nu$, $v_2/\sqrt{gr^\bullet}$

for the tangential velocity component, and similar combinations for the radial and axial velocity components also apply. The radius of the inlet boundary of this region, which varies with z is designated $r^\bullet$

6-4 Average Velocity Components

Based on the dimensional analysis presented in section 6-3, the computer program developed evaluated the powers of the terms in equations 6-3-2 and 6-3-3

a- Tangential Flow region (II)

Equation 6-3-2 takes the form;

$$6\text{-}4\text{-}1 \qquad v_2/v_* = K\ (ro/r_*)^{0.37}(z/r_*)^{0.02}(h/r_*)^{0.04}\ (Re_*)^{0.33} /[(F_*)^{0.59}\ (r/r_*)^{1.0}(b/r_*)^{0.04}]$$

It was suggested in Chapter Four that the variation in the tangential velocity component with height above the base could be

neglected in this region. This view is confirmed by the low power of z/r_* produced by the above analysis. An equivalent argument could be applied to b/r_* and h/r_* whose indices are almost similar.

In this region it was postulated that the flow is almost wholly tangential, and an analysis of the velocity yields the following relationship;

$$\Gamma_2/\Gamma^* = (r/r_*)^{0.01} \qquad 6\text{-}4\text{-}2$$

This confirms that within this region circulation is constant, and that the effect of the remaining variables in equation 6-4-1 is negligible.

The average error in equations 6-4-1 and 6-4-2 was 5.5% and 6.6%.

b- Accelerating Flow region (III)

Due to the complexity of the flow patterns adjacent to the outlet the relations obtained for the radial and axial velocity components are of necessity less accurate. Equation 6-3-3 for the radial velocity component takes the following form;

$$u/v^\bullet = K\,(ro/r^\bullet)^{0.64}(z/r^\bullet)^{-0.51}(h/r^\bullet)^{0.08} \Big/ [(F^\bullet)^{0.35}(Re^\bullet)^{0.80}(r/r^\bullet)^{2.16}(b/r^\bullet)^{0.09} \qquad 6\text{-}4\text{-}3$$

The common boundary between the Tangential Flow and Accelerating Flow regions had to be established tentatively before a more accurate assessment could be made using only relevent data points. Two conditions to be satisfied in the determination of $r^\bullet$ at heights z were;

(i) the circulation was significantly less than Γ^*

(ii) an inward radial velocity component was discernable.

For the axial velocity component, equation 6-3-3 takes the following form

$$w/v^\bullet = K\ (ro/r^\bullet)^{1.77}(z/r^\bullet)^{-0.68}(h/r^\bullet)^{0.3}(b/r^\bullet)^{0.3} \Big/ [(F^\bullet)^{0.82}(Re^\bullet)^{0.70}(r/r^\bullet)^{2.06} \qquad 6\text{-}4\text{-}4$$

Finally for the tangential velocity component, equation 6-3-3 becomes;

$$v_3/v^\bullet = K\ (ro/r^\bullet)^{0.09}(z/r^\bullet)^{0.02}(Re^\bullet)^{0.03} \Big/ [(F^\bullet)^{0.10}(h/r^\bullet)^{0.02}(r/r^\bullet)^{0.85}(b/r^\bullet)^{0.00} \qquad 6\text{-}4\text{-}5$$

In terms of circulation

$$\Gamma_3/\Gamma^\bullet = (r/r^\bullet)^{0.15} \qquad 6\text{-}4\text{-}6$$

Hence circulation varies throughout this region, and consideration of the indices in equation 6-4-5 confirms that as for Region II, other variables are unimportant.

The error in equations 6-4-3 and 6-4-4 was 19.9% and 17.0% Whilst the error in equations 6-4-5 and 6-4-6 was 5.2% and 5.4%. Figures 6-4-1,2,3 and 4 show the comparisons of the calculated values of the tangential velocity component in the Tangential Flow region (II), and radial, axial and tangential velocity components in the Accelerating Flow region (III) with the measured data .

The above dimensionless equations 6-4-1 and 6-4-5 relate the tangential velocity component in each region to its initial inlet boundary conditions. For the region of Accelerating Flow, the data were re-assessed using the initial boundary conditions to the Tangential Flow region and the following relationship resulted

$$6\text{-}4\text{-}7 \quad v_3/v_* = K\ (ro/r_*)^{1.04}(z/r_*)^{0.11}(h/r_*)^{0.12}\ (Re_*)^{1.23} /[(F_*)^{1.82}\ (r/r_*)^{0.86}(b/r_*)^{0.09}]$$

The constants K in equations 6-4-1 to 7 are obviously different in each equation, and their individual numerical values are tabulated in table 6-8-1.

6-5 Velocity Fluctuations u',v',w'

Figures 6-5-1 to 6-5-9 are some selective plots of radial and tangential velocity fluctuations. These figures show that the ve-

locity fluctuations are very significant adjacent to the air core but decrease rapidly with increasing radius. It is also noticeable that the fluctuation in the radial velocity component decreases rapidly with height above the base.

6-6 Reynolds Shear Stress ($\overline{u'v'}$) and Eddy viscosity (ε)

The values of the eddy viscosity ε together with Reynolds shear stress $\overline{u'v'}$ obtained from solving equations 4-4-5 and 4-4-2 were plotted against r and are shown in figures 6-6-1 to 23. These profiles show the effect of the Base Flow region (I) on both the Tangential Flow region (II) and the Accelerating Flow region (III), and the extent of the Accelerating Flow region radially and vertically. The steps followed in evaluating the eddy vicosity ε and consequentially Reynolds shear stress $\overline{u'v'}$ were;

a- From the experimental data of the tangential velocity component a relation was derived of the form ;

$$6\text{-}6\text{-}1 \qquad v = \Sigma_{a=1,n} \Sigma_{b=1,m} X_{a,b} (r)^a (z)^b$$

from which the first and second derivatives of v with respect to r and z were evaluated, at each set of readings. The average error in the relationship so derived was less than 0.5%.

b- The values obtained from (a) above were used in equation 4-4-4 to find F4.

c- F4 was then related to r and z in the form of equation 6-5-1 and the average error in this relation was found to be less than 0.1%.

d- Equation 4-4-5 was then solved for the eddy viscosity, ε

e- Substitution of these values of ε into 4-4-2 enabled $u'v'$ to be evaluated.

6-7 Boundary Limit r•

The radius r• at which the radial velocity component u became different from zero was defined as the boundary between the region of Tangential and Accelerating Flows. In the analyses described above , this was taken to be the actual location of a data point where the absolute value of the radial velocity component u was less than 0.5 cm/sec. The data were analysed again individually for each run, and the resulting continuous functions for $u^\bullet = f(r,z)$ were plotted in Figures 6-7-1, 6-7-2 and 6-7-3.

6-8 Geometrical Proportions

It had become apparent that the inlet and outlet conditions governed the depth, surface profiles and air core dimensions at outlet. These in turn determined whether the vortex operated with or without an air core. Four dimensionless groups relating these parameters are;

$$6\text{-}8\text{-}1 \qquad Q/(ro^{2.5}\sqrt{g}) = \psi(\Gamma^*/(ro^{1.5}\sqrt{g}) \ , \ h/ro, \ ra/ro)$$

By statistical analysis of the data, relationships between the two major dimensionless groups and each of the geometrical ratios were formulated as

6-8-2 $$Q/(ro^{2.5}\sqrt{g}) = K\ [\Gamma^*/(ro^{1.5}\sqrt{g})]^{-0.42}\ (h/ro)^{1.06}$$

and

6-8-3 $$Q/(ro^{2.5}\sqrt{g}) = K\ [\Gamma^*/(ro^{1.5}\sqrt{g})]^{0.38}\ (ra/ro)^{-1.98}$$

The error in equations 6-8-2 and 6-8-3 was 8% and 18% respectively. These curves are plotted in Figures 6-8-1 and 6-8-2 to relate with the dimensionless groups calculated from experimental data given in table 6-8. Further analysis of all the data produced a total relationship as

6-8-4 $$Q/(ro^{2.5}\sqrt{g}) = K\ (\Gamma^*/(ro^{1.5}\sqrt{g})^{-0.16}\ (ra/ro)^{-0.57}\ (h/ro)^{0.89}$$

The error in equation 6-8-4 was 6.5% .

It can be shown that the coefficient of discharge for the vortex outlet is related to $\Gamma^*(ro^{1.5}\sqrt{g})$ and hence varies with circulation. A suitable further grouping is plotted as a single curve in figure 6-8-3.

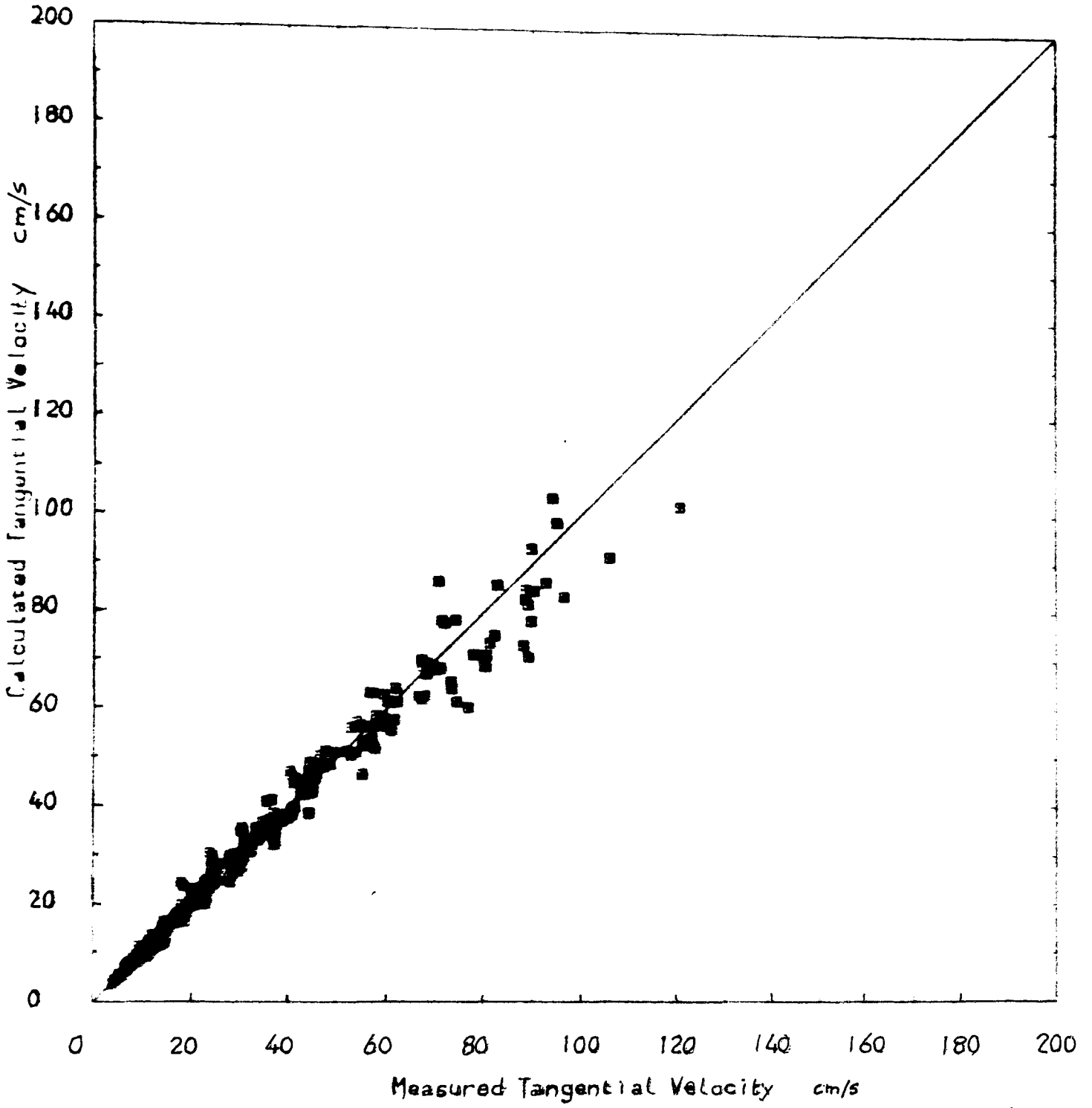

FIG. 6-4-1 Comparison between Measured and Calculated Tangential Velocity in the Tangential Flow Region (II) using EQUATION 6-4-1

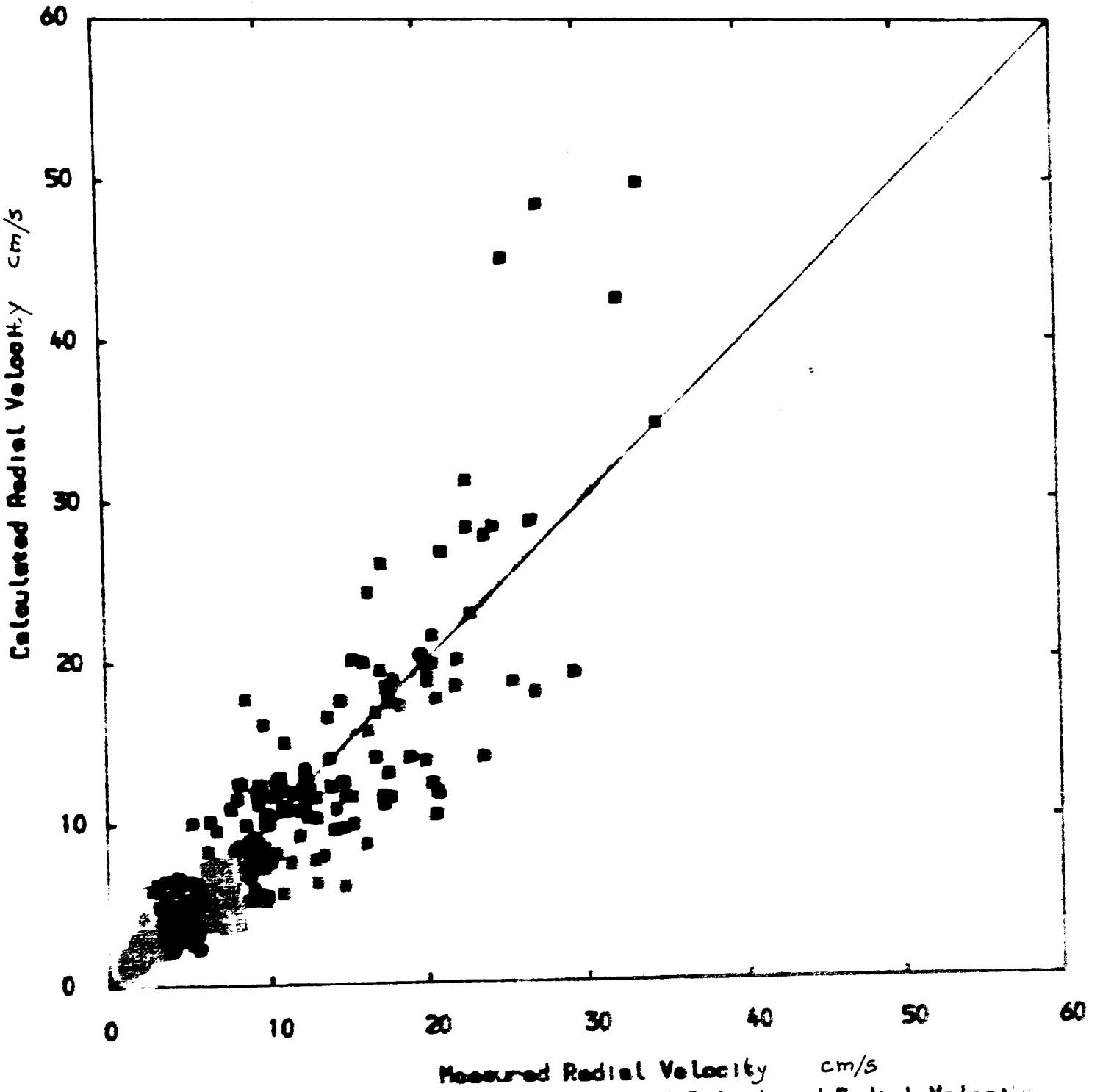

FIG. 6-4-2 Comparison between Measured and Calculated Radial Velocity in the Accelerating Flow region (III) using equation 6-4-3

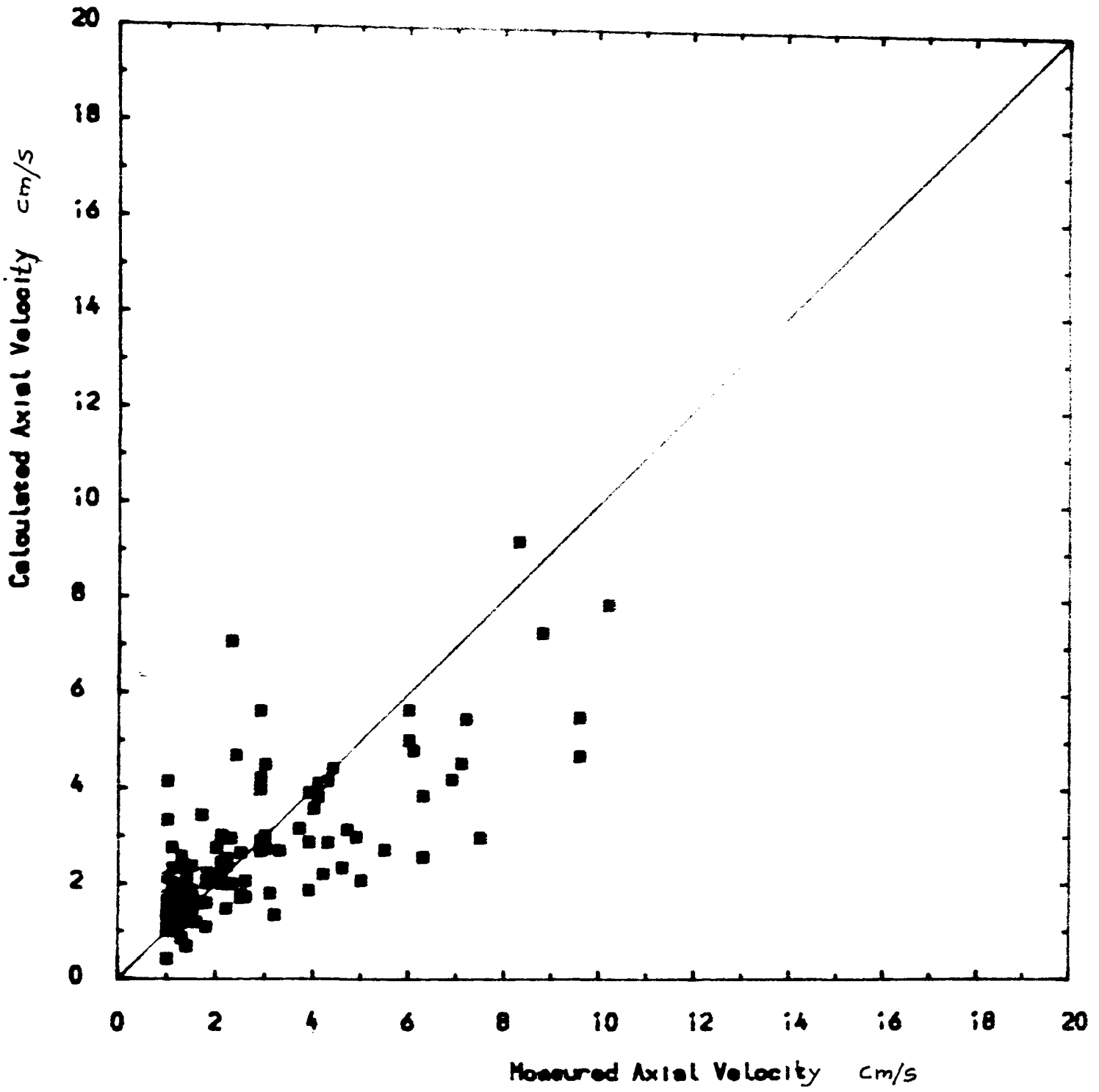

FIG. 6-4-3 Comparison between Measured and Calculated Axial Velocity in the Accelerating Flow region(III) using equation 6-4-4

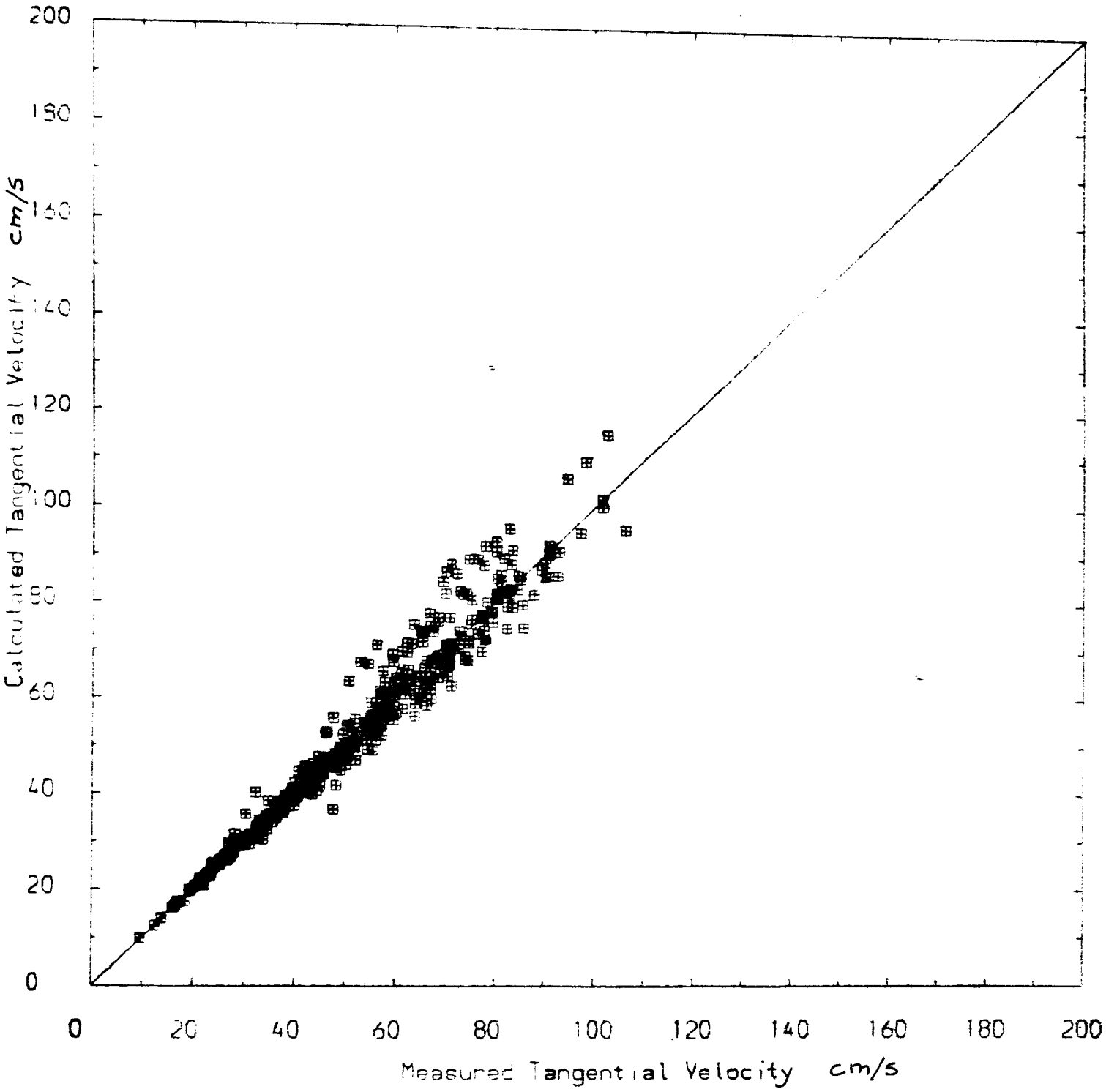

FIG. 6-4-4 Comparison between Measured and Calculated Tangential Velocity in the Accelerating Flow region(III) using equation 6-4-5

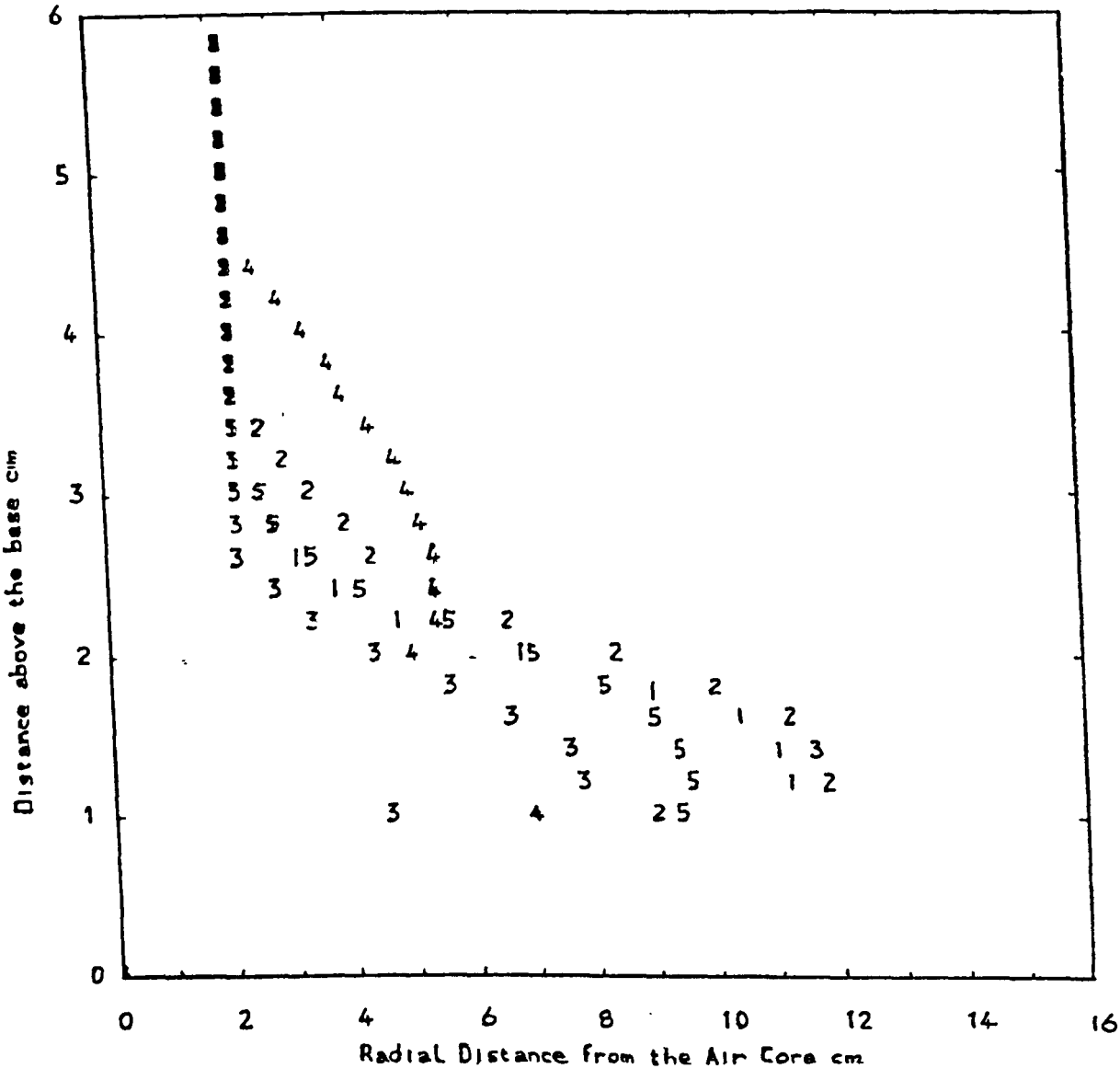

FIG. 6-7-1 Contours of the Radial Velocityu=0.5cm/sec. Pipe Diameter=28mm, 5runs

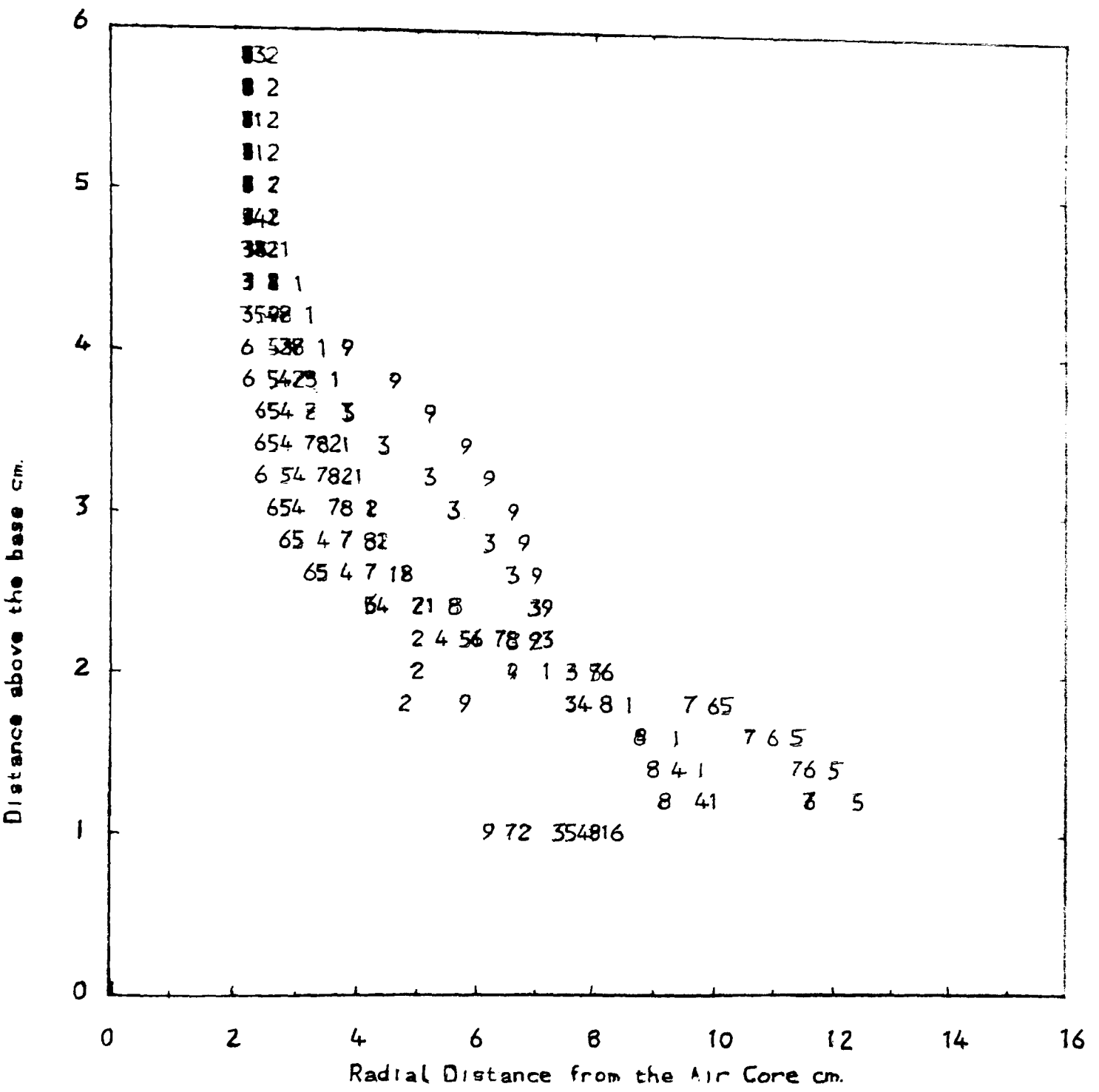

FIG. 6-7-2 Contours of the Radial Velocity u=0.5cm/sec. Pipe Diameter=38mm, 9Runs

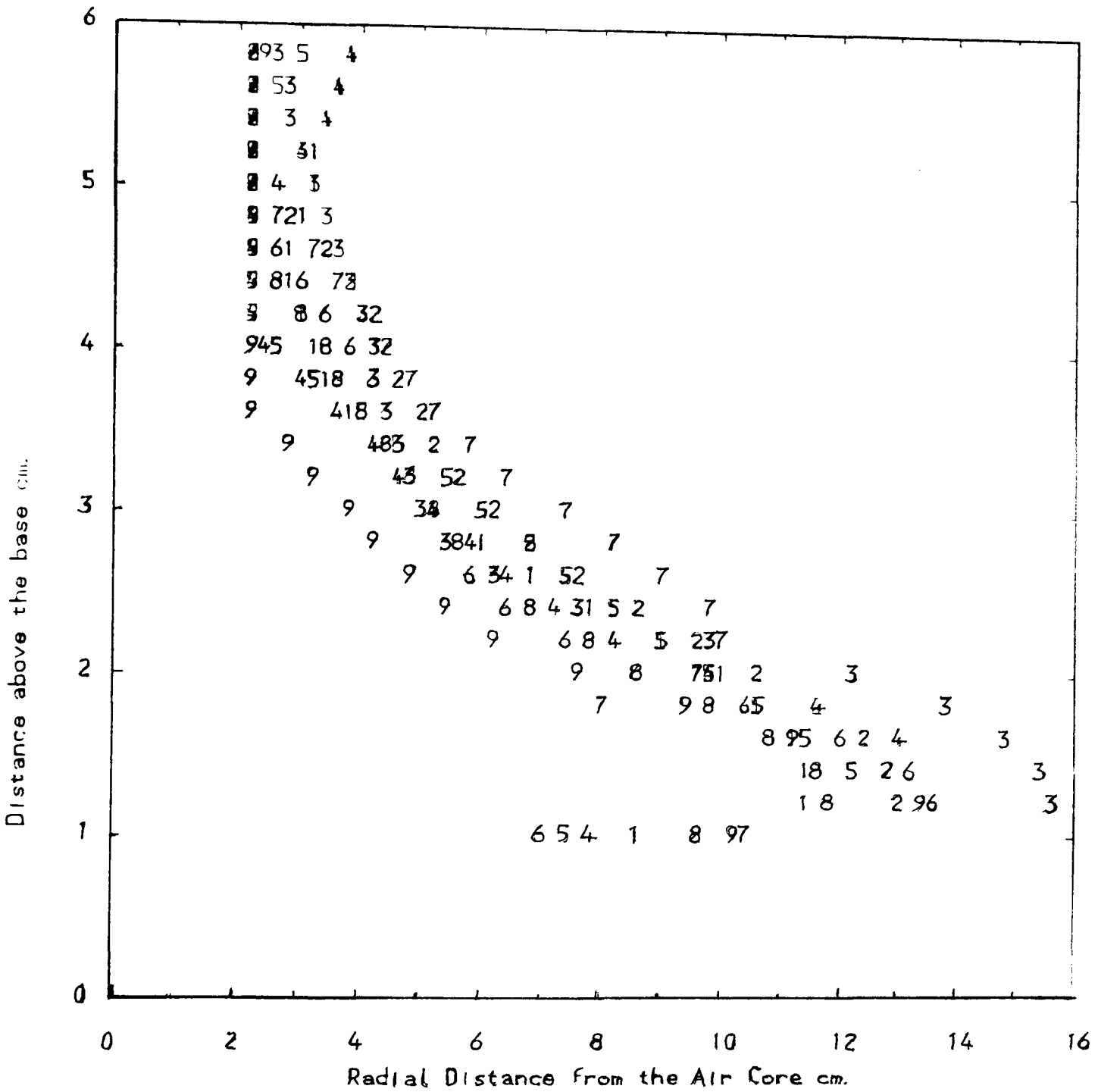

FIG. 6-7-3 Contours of the Radial Velocityu=0.5cm/sec. Pipe Diameter=53mm, 9Runs

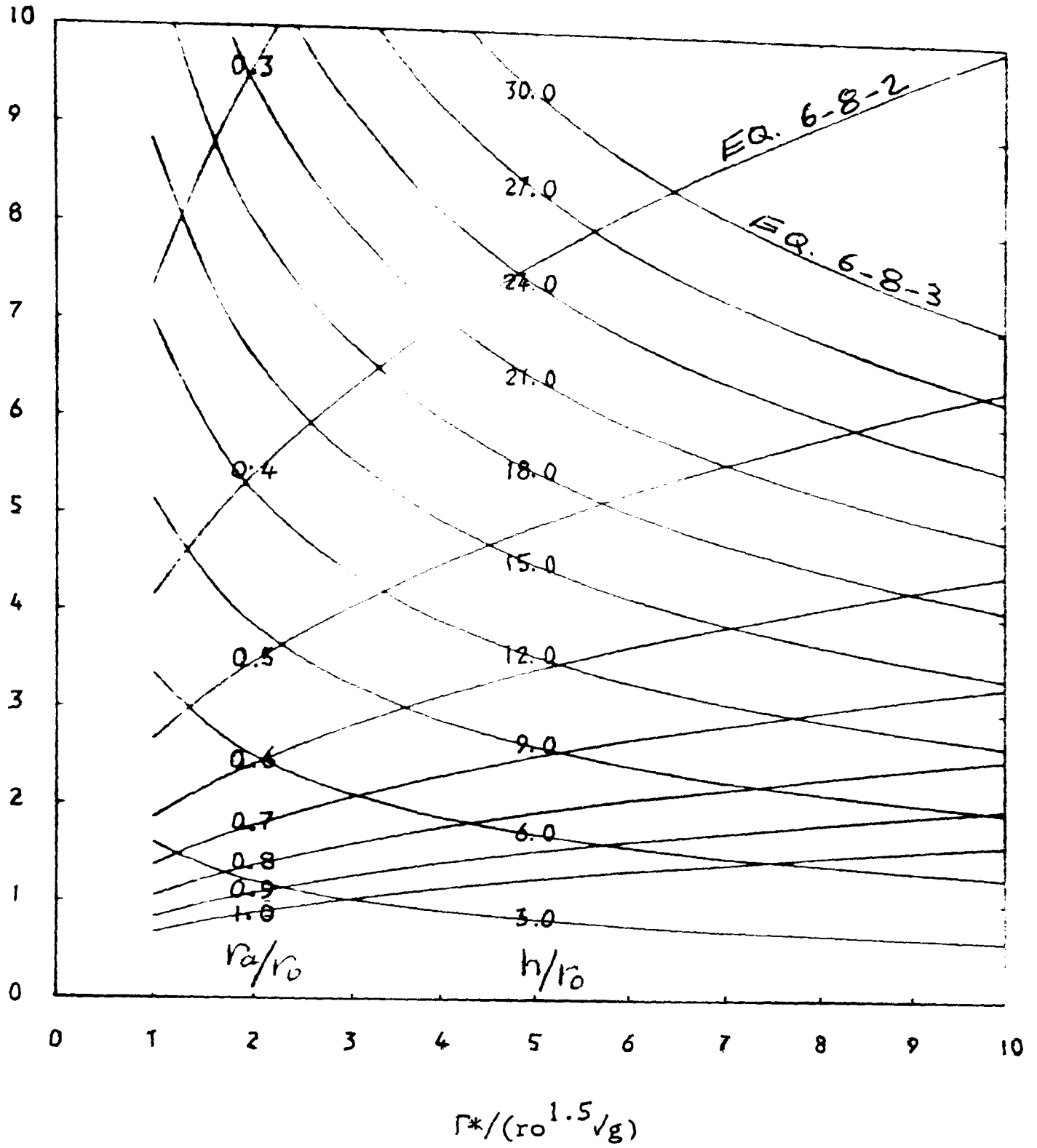

Fig 6-8-1 Dimensionless relationship given by equations 6-8-2 and 6-8-3

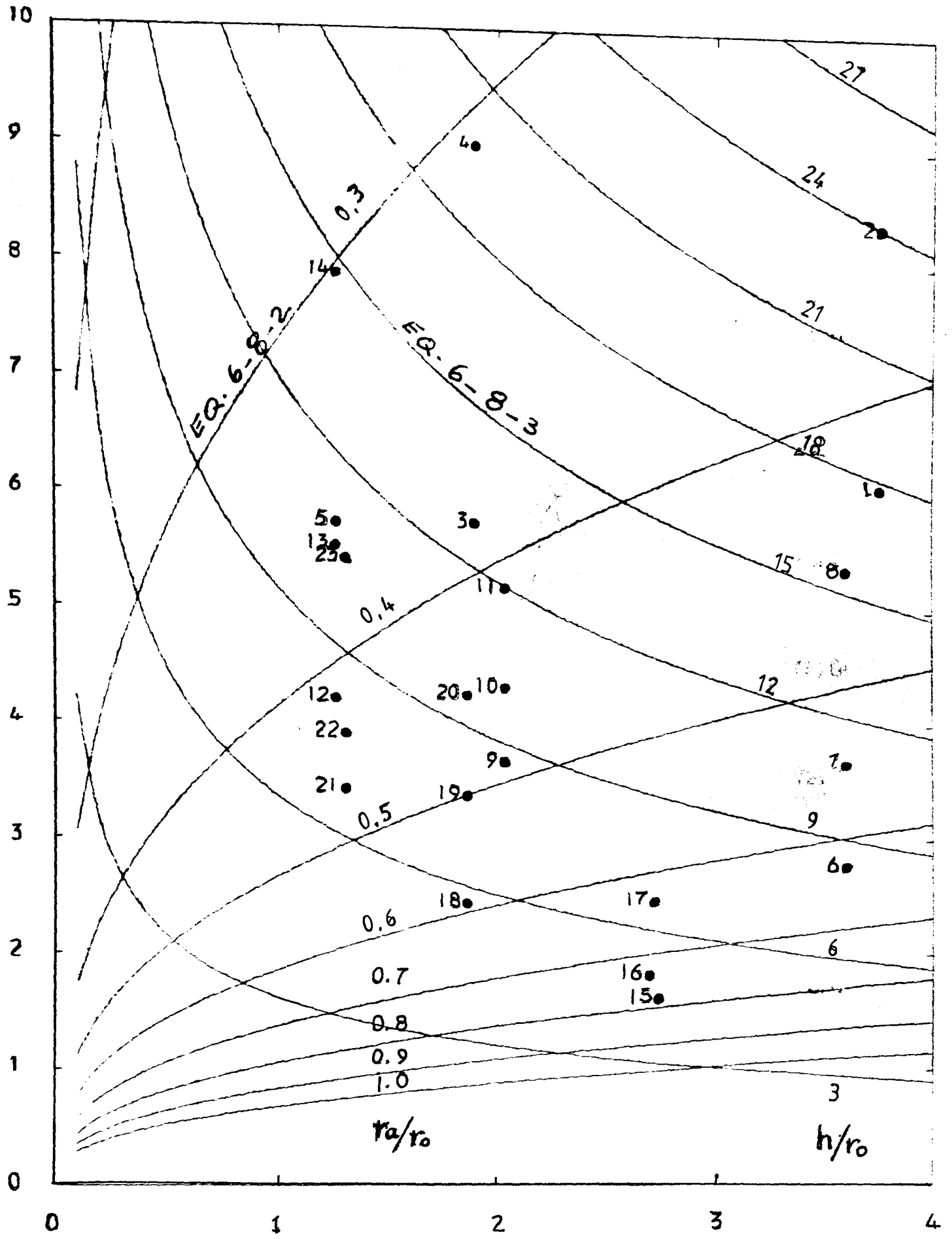

Fig. 6-8-2 Dimensionless relationship given by equations 6-8-2 and 6-8-3. showing the experimental data points.

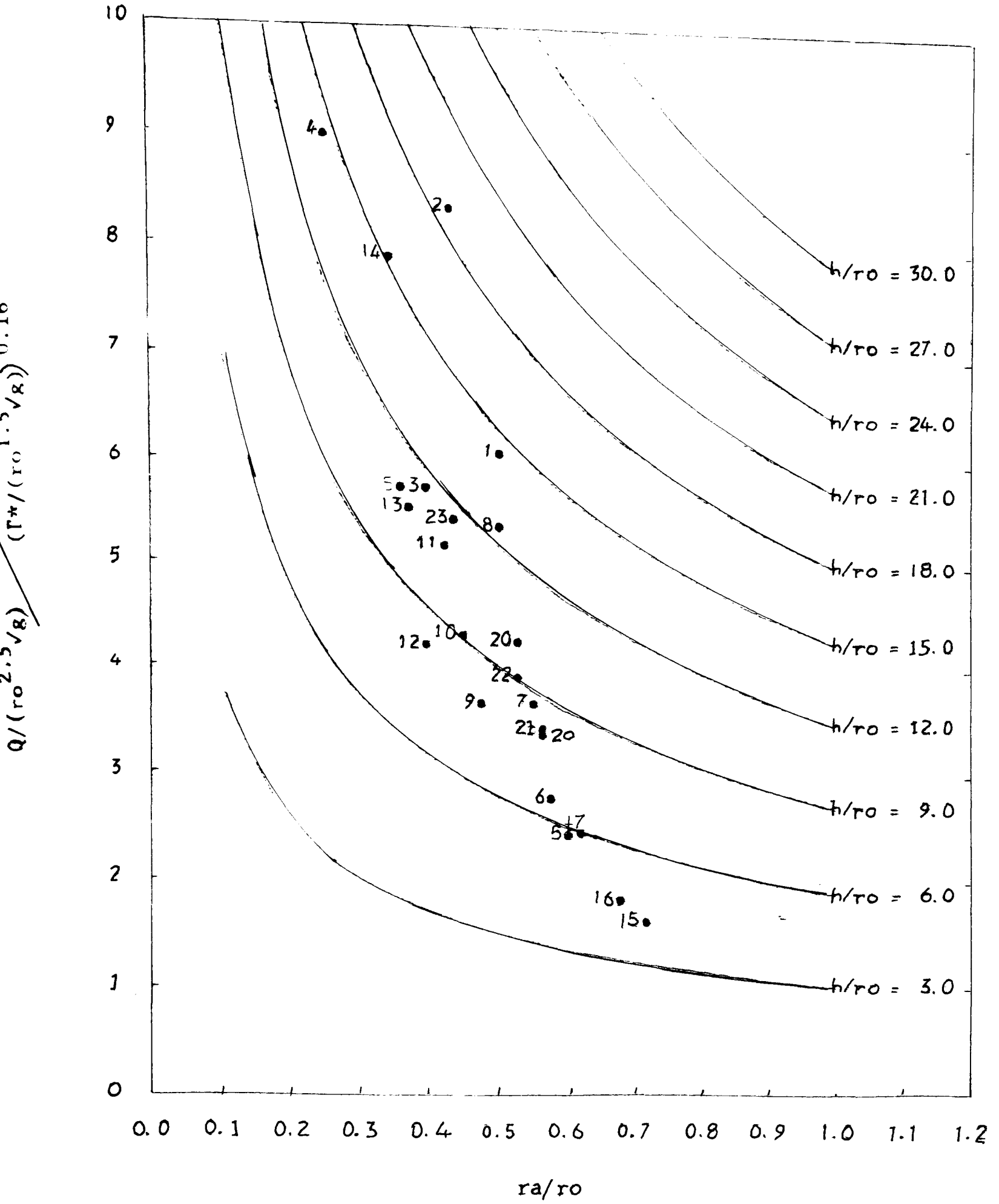

Fig. 6-8-3 Dimensionless relationship given in equation 6-8-4.

Table 6-8-1

Values of the constant K and percentage error

Equation No.	K	% error
6-4-1	$(10)^{-1.84}$	5.5
6-4-2	$(10)^{0.0}$	6.6
6-4-3	$(10)^{1.96}$	19.9
6-4-4	$(10)^{1.97}$	17.1
6-4-5	$(10)^{0.0}$	5.2
6-4-6	$(10)^{0.0}$	5.5
6-4-7	$(10)^{-6.4}$	7.9
6-8-2	$(10)^{-0.3}$	8.1
6-8-3	$(10)^{10.17}$	18.1
6-8-4	$(10)^{-0.42}$	6.5

Table 6-8-2

Vortex dimensions and parameters

	ro	ra	h	Q	Γ	Cd
1	1.400	0.700	24.000	440.640	194.820	0.330
2	1.400	0.600	33.000	605.880	194.820	0.387
3	1.400	0.550	21.000	415.800	98.100	0.333
4	1.400	0.350	33.000	653.400	98.100	0.417
5	1.400	0.500	16.000	416.000	65.000	0.381
6	1.900	1.100	15.500	431.055	295.095	0.218
7	1.900	1.050	20.500	570.105	295.095	0.251
8	1.900	0.950	30.000	834.300	295.095	0.303
9	1.900	0.900	17.000	570.350	166.225	0.275
10	1.900	0.850	20.000	671.000	166.225	0.299
11	1.900	0.800	24.000	805.200	166.225	0.327
12	1.900	0.750	16.000	656.000	102.500	0.326
13	1.900	0.700	21.000	861.000	102.500	0.374
14	1.900	0.650	30.000	1230.000	102.500	0.447
15	2.650	1.900	16.600	578.178	369.585	0.145
16	2.650	1.800	19.000	651.510	363.855	0.153
17	2.650	1.650	25.400	877.824	366.720	0.178
18	2.650	1.600	17.200	870.320	250.700	0.215

19	2.650	1.500	23.800	1204.280	250.700	0.253
20	2.650	1.400	30.000	1518.000	250.700	0.284
21	2.650	1.500	17.500	1225.000	175.000	0.300
22	2.650	1.400	20.000	1400.000	175.000	0.320
23	2.650	1.150	27.700	1939.000	175.000	0.377

	$Q/ro^{2.5}\sqrt{g}$	$\Gamma/ro^{1.5}\sqrt{g}$	h/ro	ra/ro
	---	---	---	---
1	6.069	3.934	17.143	0.500
2	8.346	3.934	23.571	0.429
3	5.727	2.083	15.000	0.393
4	9.000	2.083	23.571	0.250
5	5.730	1.504	11.429	0.357
6	2.767	3.769	8.158	0.579
7	3.660	3.769	10.789	0.553
8	5.356	3.769	15.789	0.500
9	3.661	2.232	8.947	0.474
10	4.308	2.232	10.526	0.447
11	5.169	2.232	12.632	0.421
12	4.211	1.500	8.421	0.395
13	5.527	1.500	11.053	0.368
14	7.896	1.500	15.789	0.342
15	1.616	2.866	6.264	0.717

16	1.821	2.821	7.170	0.679
17	2.453	2.843	9.585	0.623
18	2.432	2.044	6.491	0.604
19	3.365	2.044	8.981	0.566
20	4.242	2.044	11.321	0.528
21	3.423	1.555	6.604	0.566
22	3.912	1.555	7.547	0.528
23	5.418	1.555	10.453	0.434

in which ro , outlet radius (cms)

ra , air core radius at 10mm distance above the base (cms)

h , water depth at inlet (cms)

Q , flow rate at inlet (cm^3/sec)

Γ , circulation at radius R (V R) (cm^2/sec)

Cd , discharge coefficient($Q/(Ao\sqrt{2gh})$)

CHAPTER SEVEN

DISCUSSION

In this chapter section 7-1 analyses the accuracy and reproducibility of the data as measured. Section 7-2 examines the methods implemented in defining the centre of rotation. Section 7-3 discusses the behaviour of the velocity components based on the figures produced. Finally section 7-4 discusses the values of the Reynolds stresses and eddy viscosity evaluated from the mathematical approach in Chapter Four and the figures resulted from it.

7-1 Accuracy and Reproducibility

In this section the accuracy and reproducibility of the experimental results is discussed. For the purposes of the discussion, accuracy is taken to include both systematic and random errors. A systematic error biases the measured value away from the true value in a single direction, a random error introduces scatter in the measurements about a mean value. The spread of the points is usually assumed to follow a Gaussian distribution. Reproducibility is clearly assessed by the degree of similarity between sets of readings obtained from repeated measurements.

The measurements were affected by errors in the position of the measuring volume, in the instrumentation, and in the fringe

spacing and orientation with respect to the flow. The predominant source of error in the measuring volume position was a systematic error. The flow rates measured using a stop watch and volumetric tank were checked by the readings of a differential water monometer connected to an orifice meter in the water supply pipe; a basic 1 to 2% uncertainity could be assumed.

The uncertainty in water depth measurements could be taken as 0.1% with 1 to 2% error due to change in water depth during data collection.

Doppler frequency measurements were affected by errors introduced by the electronic processing instruments including the frequency Tracker and frequency Shifter. From the manufacturer's specifications, the accuracy of the analog output over the operating range varied between 1.0% to 1.2% of full scale deflection.

The accuracy with which the velocity components could be determined included, in addition to error in the Laser Doppler Anemometer reading, an error in the exact location of the centre of rotation. From figures 5-5-1a to 5-5-24a which were produced from figures 5-5-1 to 5-5-24, it is clear that the velocity gradient is large near the outlet and 1mm error in locating the centre of rotation may yield to up to 15% error in the velocity estimate.

7-2 Centre of Rotation

The two methods explained in section 5-5 to determine the centre of rotation checked each other. From the first method ex-

plained in section 5-5 figures 5-5-1 to 5-5-24 were plotted. The lines of equal velocity are shown in figures 5-5-1a to 5-5-24a. These lines are:

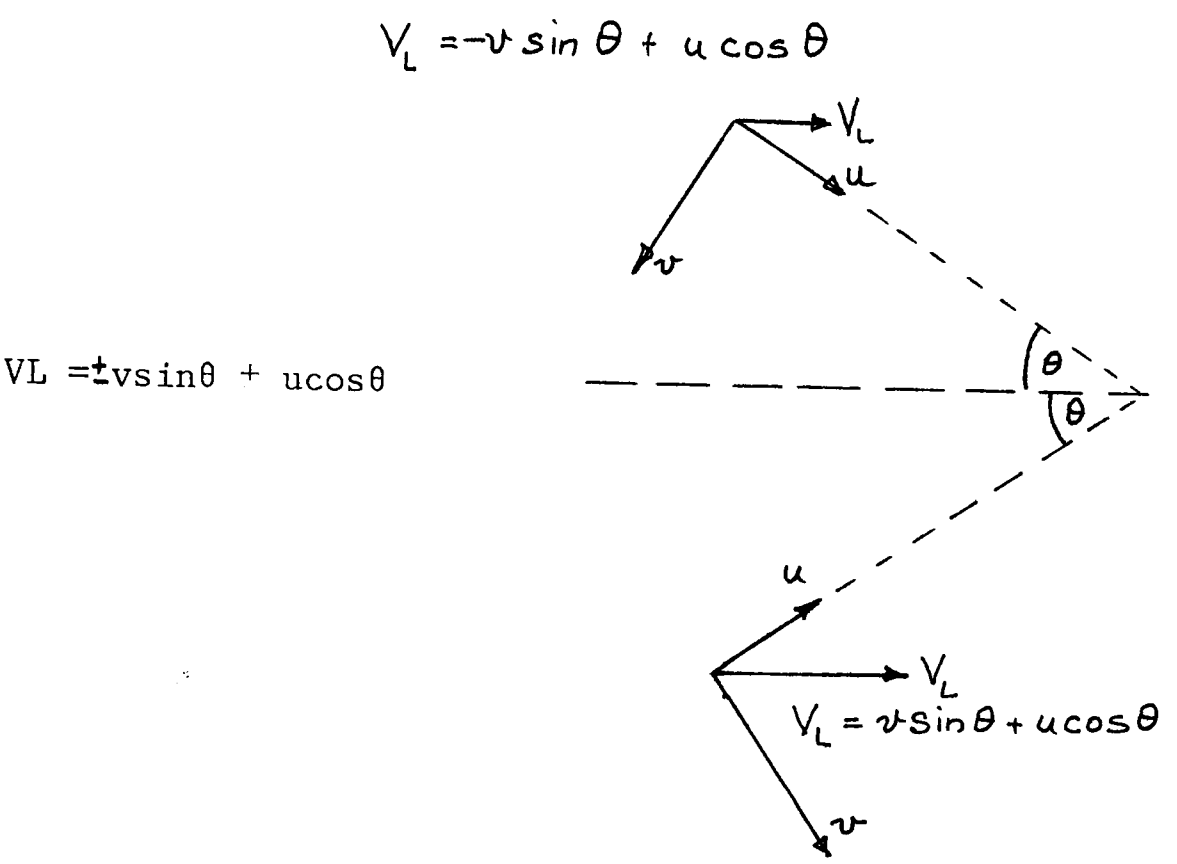

VL = ±vsinθ + ucosθ

The line of zero velocity VL being always located in the negative region meant that there was a radial velocity component toward the outlet and, its value was

$$u = v\sin\theta/\cos\theta = v \tan\theta$$

These lines of equal value of VL show clearly that the radial velocity component decreases outward from the outlet and also decreases with increase in the distance above the base.

The profiles of the velocity VL normal to the laser beam are shown in figures 5-5-1 to 24. These profiles clearly show that at a radius of 1.5cm the variation of the velocity measured showed distinct differences from those at other radii. These measurements were within the diameter of the outlet pipe, and it had been anticipated that some differences were likely in this region.

7-3 Velocity Components

From figures 6-2-7 to 29 it is apparent that for quite significant reductions in radius the radial velocity component which is initially negligible changes little. For the same region the tangential velocity increases, but there is no significant variation in velocity with height above the base. At some radius, variations in the tangential velocity with height above the base become apparent, and also a radial velocity component is observed. The minimum radius at which velocities were measured was within the diameter of the outlet pipe, hence these points were within the Core Flow region, and do not necessarily maintain the trends shown in the region of Accelerating Flow region (III).

7-4 Reynolds Stresses and Eddy Viscosity

The values of Reynolds stresses and eddy viscosity determined by using measured velocities to solve the suitably approximated form of the Navier Stokes equations equation 4-3-21 when plotted against radial distance and at various heights above the base show

variations similar to the variations in the tangential and radial velocity component, figures 6-6-1 to 6-6-23.

Figures 6-6-1a to 6-6-23a and 6-6-1b to 6-6-23b are contours of the eddy viscosity and Reynolds stress developed from figures 6-6-1 to 6-6-23.

CHAPTER EIGHT

CONCLUSIONS

8-1 Flow Regions

From the experimental results tabulated in Tables (5-6-1 to 5-6-6) and plotted in figures (6-2-1 to 6-2-29), it appears that within the boundaries where velocity measurements were made, as predicted in Chapter Four, there exist two regions in which the flow classication are distinctly different. These are:

1- An outer region is shown by figure (4-4-1) in which the radial velocity component is negligible, and the tangential velocity component increases inversely with radius approximately as a free vortex. This was referred to in Chapter Four as a region of Tangential Flow (II).

2- A zone confined between the outlet pipe and the above region , in which increasing radial accelerations occur. The tangential velocity component decreases from that predicted at constant circulation. This was previously designated in Chapter Four as the Accelerating Flow region(III).

8-2 Tangential Flow Region

It was observed during experimental runs that for a constant flow rate Q, and fixed inlet conditions, the depth in the vortex

chamber decreased as the diameter of the outlet pipe increased. For a given outlet pipe diameter, and fixed inlet conditions, it was established that the flow rate Q was almost directly proportioned to the depth of water in the vortex chamber h. Hence the inlet velocity was constant for each inlet geometry tested, and only varied with outlet pipe diameter. Analysis showed the results were related by equation 6-4-1

$$6\text{-}4\text{-}1 \qquad v_2/v_* = K\ (ro/r_*)^{0.37}(z/r_*)^{0.02}(h/r_*)^{0.04}\ (Re_*)^{0.33} / [(F_*)^{0.59}\ (r/r_*)^{1.0}(b/r_*)^{0.04}]$$

which confirms the validity of the direct observations made.

The height z above the base, breath at inlet b and water depth at inlet h were also included as variables when formulating the possible dimensionless groups, but the indices of the resulting geometric ratios produced by the statistical analysis of the results were only 0.02,-0.04 and 0.04 respectively as indicated in equation 6-4-1. It is justified to omit these non-dimensional groups, as having little bearing on the velocity v_2 within this region. Hence the velocity v_2 at any radius r and height z is given by equation

$$8\text{-}2\text{-}1 \qquad v_2/v_* = K\ (ro/r_*)^{0.18}(Re_*)^{0.28}\ (F_*)^{-0.42}(r_*/r)^{1.0}$$

This equation is thus shown to be applicable for the evaluation of the tangential flow variations within this region. Further analysis to investigate variations in circulation resulted in equation 6-4-2 which confirms that circulation is in fact constant.

It is thus shown that free vortex flow conditions apply, determined by both inlet and outlet conditions. It was also established that the radial and axial velocity components within the body of this region were insignificant.

The data collected in this region are plotted in figure 6-4-1 against values predicted by equation 6-4-1. The number of data point is in excess of 1000, and the plotting confirms the relevence of the above relationships.

8-3 Accelerating Flow Region

Analysis of the data into the suggested dimensionless groupings given in equation 6-3-3, resulted in equation 6-4-5

6-4-5 $$v_3/v^\bullet = K\ (ro/r^\bullet)^{0.09}(z/r^\bullet)^{0.02}(Re^\bullet)^{0.03} / [(F^\bullet)^{0.10}(h/r^\bullet)^{0.02}(r/r^\bullet)^{0.85}(b/r^\bullet)^{0.00}$$

Omitting the relatively unimportant groups, the above equation reduces to

8-3-1 $$v_3/v^\bullet = K\ (r^\bullet/r)^{0.85}$$

equation 8-3-1 is identical to equation 6-4-6

This clearly indicates that the circulation is no longer constant as in the region of Tangential Flow, but varies with r and z. In this equation r• is the radius at which the radial velocity vector is consistently towards the outlet, and hence the fluid particles at this radius commence a spiral motion towards the central outlet.

Comparison of the values obtained from equation 6-4-5 with actual measured data plotted in figure 6-4-4 shows that even in the very rapidly changing flow regimes adjacent to the outlet, a high degree of correlation of the proposed relationships has been attained. These are based on measurements at more than 600 separate locations.

There are significant differences in the circulation patterns within the two regions, as shown by comparison of equations 6-4-2 and 6-4-6.

Further examination of the indices of the parameters involved as given in equations 6-4-1 and 6-4-7 shows that there are distinct differences in the degree of dependence of the tangential velocities on viscous and gravitational parameters and geometrical ratios.

The radial velocity component in this region increases rapidly from the common boundary with the region of Tangential Flow, at-

tains a peak value, and decreases to zero at the air core. Vertically the radial velocity component at any radius is also zero at the base, increases rapidly, and again decreases to zero at the common boundary with the Tangential Flow region.

On any vertical section, the velocity vector at the common boundary between this region and the Tangential Flow region is very nearly tangential, whilst near the base it becomes almost radial, these changes occuring in a vertical distance of no more than 5cm.

8-4 Reynolds Stress $\overline{u'v'}$ and eddy viscosity ε

Comparison of the plotted evaluations of the eddy viscosity ε and Reynolds stress $\overline{u'v'}$ given in figures 6-6-1,1a,1b to 6-6-23,23a,23b shows that the physical size of the Accelerating Flow region varies both with flow rate Q, and with initial circulation. Examination of figures 6-6-6a,7a,and 8a which are under the same geometric conditions with flow rates of 0.431/sec,0.571/sec and 0.831/sec. shows that the location of the contour lines at $\varepsilon = 2.$ differ for each flow. The same effect is also noticed in figures 6-6-7a and 6-6-9a which are for the same flow rate but initial circulations of 300.0 cm^2/sec and 180.0 cm^2/sec.

8-5 Geometrical Proportion

Analysis of the data relating flow rate, circulation and air core diameter to the geometrical properties of the vortex chamber was shown in section 6-8, and the experimental data were plotted

against derived relationships in Figures 6-8-1, and 6-8-2. These charts confirm the earlier opinions that any change in either flow rate or circulation, or outlet diameter will demand some change in the depth at entry to the vortex chamber, and percentage air core.

It is thus established that for a given geometry and outlet diameter, any change in flow rate or circulation will be accompaned by changes in depth and air core, the limiting case being zero air core. A further increase in flow rate results in a rapid draw down in the vortex chamber and violent surging.

8-6 Comparison with Previous Reports

No previous investigators have defined the proposed region of Accelerating Flow in any detail, even though they have recognizes that rapid velocity changes occur adjacent to the outlet. The following comparison are therefore made with the current findings in the region of Tangential Flow.

Reports contained in refrences (Einstein & Li 1955, Holtorff 1964, Anwar 1965,1967 and 1969, and Granger 1966) have claimed that the flow patterns do not change significantly with the height above the base. The present work corroborates their findings in this respect.

In addition it is agreed that circulation, away from the base and the sides is relatively constant, and that the axial and radial velocity components are negligible (Holtorff 1964)

Stevens and Kolf 1957 assumed for mathematical convenience that a radial velocity existed throughout the vortex, but except in designated regions this was not found to be so.

In the Accelerating Flow region, Dagget 1974 shows that the radial velocity increases towards the outlet, reaching a maximum at 1.5ro. The current work shows that this occurs more nearly at 1.0ro. He also shows circulation to be constant, whereas some of the kinetic energy of rotation must be taken to provide radial accelerations. That this is the case has been established by the present work, and also shown by Anwar 1969.

Estimations of eddy viscosity in this region, confirmed that the suggestion made by Anwar 1969 that Reynolds stress is proportional to the rate of strain resulated in positive values, whilst Prandtl's proposal showed ε to be negative. Einstein and Li 1955 proposed ε to be constant in order to facilitate the solution of the basic equations. The relations developed with experimental work which was mainly in laminar flow conditions awarded equal prominence to ν and ε. The present work confirms the more widely held opinion that in general $\varepsilon >> \nu$, and is variable within the same flow region.

The comments made by Zilinski 1968, Dagget 1957, and Anwar1980 and 1983 regarding geometrical ratios on cofficient of discharge, circulation, depths and air cores are also generally confirmed.

8-7 Achievements and recomendations for further investigation

The investigation was initiated to develop a clearer understanding of the important flow parameters in the region of a vertical outlet from a free vortex with stable air core. Previous researchers have claimed the existance of several different flow regions, and this research utilised divergences from classical hydrodynamic theories, as definitions of the boundaries of separation.

Existence of Reynolds stresses, and eddy viscosities evaluated from velocity traverses to measure mean and fluctuating components are used to indicate the presence of a region of Accelerating Flow. More direct analysis of the data using only dimensional considerations, also confirmed the above.

Dimensional techniques applied to the overall engineering aspects of these vortices, showed that the four relevent diminsionless groupings are uniquely related.

Whilst not providing complete understanding of the total phenomena , these results can be an important guide to the design limits of vortices in civil engineering.

Further work is necessary using 2/3 component laser techniques to directly assess the turbulent quantities within the region of Accelerating Flow indicated in this work. The present work was carried out using an apparatus with smooth surfaces, whilst

boundary layer effects near the outlet appear to determine the extent of this region.

The necessary further clarification would be obtained using roughened surfaces adjacent to the outlet.

The limits of the general geometrical proportions of the vortex at collapse of air and subsequent surging were not determined, and further work is also necessary if relevent design criteria are to be precisely quantified.

REFERENCES

AHMED, M.; WIGELAND, R.A. & NAGIB, H.N. 1976 Enqu'ete Sur La Formation de Vortex et autres Anomalies D'e'coulement dans une Enceinte avec ou sans Surface Libre. La Hoville Blanche, No.1,3-40.

AMPHLET, M.B. 1976 Air-Enraining Vortices at a Horizontal Intake. Hydraulic Research Station Report No. OD/7 April.

AMPHLET, M.B. 1978 Air-Entraining Vortices at a Vertically Inverted Intake. Hydraulic Research Station Report No.OD/17 Sept.

ANWAR, H.O. 1965 Coefficient of Discharge for Gravity Flow into Vertical Pipes. Journal of Hydraulic Research -3- No.1.

ANWAR, H.O. 1966 Formation of Weak Vortex. Journal of Hydraulic Research -4- No.1.

ANWAR, H.O. 1967 Vortices at Low-Head Intakes. Water Power Nov., 455.

ANWAR, H.O. 1969 Turbulent Flow in a Vortex. Journal of Hydraulic Research -7- Part 1.

ANWAR, H.O.; WELLER, J.A. & AMPHLET, M.B. 1978 Similarity of Free Vortex at Horizontal Intake. Journal of Hydraulic Research Vol.16 No.2-95.

ANWAR, H.O. & AMPHLET, M.B. 1980 Vortices at Vertically Inverted Intake. Journal of Hydraulic Research Vol.18,No.2 ,123.

ANWAR, H.O. 1983 The Non-Dimensional Parameters Of Free-Surface Vortices Measured for Horizontal and Vertical Intakes. LAHOULLE BLANCHE No.1-10.

BARLOW, J.B. 1972 Measurement of Wing Wake Vorticity for Several Spanwise Load Distributions. University of Maryland Report.

BERGE, J.P. 1961 E'tudes des Phe'nome'nes de Vortex dans un Liquide a' Surface Libre-Recherche et Mise au Point d'um Nouveau Crite're de Comparaison. Center de Recherche et d'Essais de Chatou,Nov.

BERGE, J.P. 1965 E'tudes des Phe'nome'nes de Vortex dans un Liquide a' Surface Libre: Me'thodes Optiques Expe'rimentales d'e'tude. B. Center de Recherche et d'Essais de Chatou,No.13,3-23.

BERGE, J.P. 1966 Enque'te sur La Formation de Vortex et autres Anomalies D'e'coulement dans une Enceinte avec ou sans Surface Libre. La Hoville Blanche,No.1,3-40.

DAGGETT, L.L. & KEULEGAN, G.H. 1974 Similitude in Free-Surface Vortex Formation. Journal of Hydraulic Division Proc.ASCE. Vol.100-Hy11. Nov.,1565.

DENNY, D.F. & YOUNG, G.A. 1957 The Preventation of Vortices and Swirl at Intakes. BHRA No.SP583.

DURST, F.A.; MELLING, A. & WHITELAW, J.H. 1981 Principles and Practice of Laser-Doppler anemometery. Academic Press- Second eddition.

ECKELMANN, H. ; HYCHAS, S.G. ; BRODLCEY, R.S. & WALLACE, J.M. 1977 Vorticity and turbulence Production in a Pattern Recognized turbulent Flow Structures. Physics of Fluids Vol.20 No.10.

ENSTEIN, H.A. & LI, H. 1955 Steady Vortex Flow in a Real Fluid. La Houille Blanche Vol.21,Part1,13.

FOSS, J. 1979 Transverse Vorticity Measurements. Dynamic flow Conference, Marseille/Baltimore. Proceeding, Alphen aan den Rijn, The Notherlands, Sijthoff & Noordhoff,983-1001.

GRANGER, R. 1966 Steady Three-Dimensional Vortex Flow. Journal of Fluid Mechanics Vol.25 Part3,557.

HOLDEMAN, J.D. & FOSS, J.F. 1975 The Initiation, Development and Decay of the Secondary Flow in a Bounded Jet. Journal of Fluids Engineering Vol.97 Series I, No.3,342-352.

HOLTORFF, G. 1964 The Free Surface and The Conditions of Similitude for a Vortex. La Houille Blanche Vol.19 part3,377.

JAIN, A.K. RATJU, K.G.R. & GARDE, R.J. 1978 Vortex Formation at Vertical Pipe Intake. Journal of Hydraulics Division Proc.ASCE. Vol.104 -Hy10,1429.

KISTLER, A.L. 1952 The Vorticity Meter. M.Sc. Thesis The Johns Hopkins University.

LEVI, E. 1972 Experiments on Unstable Vortices. Journal of Mechanical Division Proc. ASCE. Vol.98-EM3.

LEWELLEN, W.S. 1962 A Solution for Three-Dimensional Vortex Flows with Strong Circulation. Journal of Fluid Mechanics Vol.14,420.

LEWELLEN, W.S. 1976 Theoretical Models of the Tornedo Vortex. Symposium on Tornedos, Lubbock, Texas, june. Texas Technical University, 107.

MACAGNO, E.O. 1969 Flow Visualization in Liquids. IIHR Report No.114, Institute of Hydraulic Research, The University of IOWA, IOWA City.

MARRIS, A.W. 1976 Theory of the Bath Tub Vortex. ASME Paper No.66 -WA/APM-11, Nov./Dec.

McCORMICK, B.W. ; TANGLER, J.L. & SHERRIEB, H.E. 1968 Structure of Trailing Vortices. Journal of Aircraft Vol.5 , 260, March.

ROTT, N. & LEWELLEN, W.S. 1966 Boundary Layers and their Interactions in Rotating Flows. Prog. Aeronout. sci. 7,557.

SEDDON, A.E. & ANWAR, H.O. 1963 Measuring Fluid Velocities Optically, Engineering Vol.6, 318.

SHAPIRO, A. 1974 Illustrated Experiments in Fluid Mechanics. MIT press.

SHARP, J.J. 1981 Hydraulic Modelling. Butterworth.

STEVENS, J.C. & KOLF, R.C. 1957 Vortex Flow Through Horizontal Orifice. Journal of Sanitary Division Proc.ASCE. Vol.83 No.SA6 Paper No.1461.

VAN DYKE, M. 1964 Peturbation Methods in Fluid Mechanics, Academic, New York .

WERLE, H. 1963 M'ethodes de Visualisation des E'coulements Hydrauliques. La Hovill Blanche, No.18,587-595

WIGELAND, R.A.; AHMED, M. & NAJIB, H.M. 1977 Vorticity Measurements Using Calibrated Vane-Vorticity Indicators and Comparison with Cross- Wire Data. AIAA Tenth Fluid and Plasma Dynamics Conference, Alburquerque, N. Maxico.

WILLMARTH, W.W. 1979 Nonsteady Vorticity Measurements: Survey and New Results. Proceeding; Dynamics Flow Conference 1978: Dy-

namic Measurements in unsteady Flows, Sijthoff and Noordhoff, Alphen aan den Rijn, The Netherlands, 1003-1012.

WYNGAARD, J. 1969 Spatial Resolution of the Vorticity Meter and other Hot-Wire Arrays. Journal of Scientific Instruments,Ser.2,Vol.2.

YANG, W.J. 1983 Flow Visualization III. Proceeding of the Third International Symposium on Flow Visualization, September 6-9, University of Michigan, Ann Arbor, Michigan, USA.

ZALAY, A.D. 1976 Hot-Wire and Vorticity Meter Wake Vortex Surveys. AIAA , Vol.14, No.5,694-696.

ZIELINSKI, P.B. & WILLEMONTE, J.R. 1968 Effect of Viscosity on Vortex Orifice Flow. Journal of Hydraulic Division Proc.ASCE. Vol.94 HY3,745.